ECONOMICAL CONCRETE MIX DESIGNS FOR HIGHWAY APPLICATIONS WITH A HIGH DOSAGE OF FLYASH

by

Rimpal V. Shah

A Thesis Presented in Partial Fulfillment
of the Requirements for the Degree
Master of Science

ARIZONA STATE UNIVERSITY

August 2003

ECONOMICAL CONCRETE MIX DESIGNS FOR HIGHWAY APPLICATIONS

WITH A HIGH DOSAGE OF FLYASH

by

Rimpal V. Shah

has been approved

July 2003

APPROVED:

_____, Chair

_____

_____

_____

Supervisory Committee

ACCEPTED:

_____

Department Chair

_____

Dean, Graduate College

ABSTRACT

The study of the mechanical properties of concrete with blended coal flyash and concrete reinforced with Alkali Resistant (AR) glass fibers is presented in this thesis. The effect of increasing blended coal flyash content up to 30% in the paving concrete was studied. Various mixes were developed for paving concrete, which aimed to meet the required specifications provided by the Arizona Department of Transportation (ADOT). To address the strength and toughness, both closed-loop compression and flexure tests were conducted. The results were compared with the control specimens prepared using the current mix design procedures of the ADOT. Finally, these mix designs were implemented in a field trial. The fibers were used in order to increase the strength and toughness properties in the concrete. The High Dispersion (HD) and the High Performance AR glass fibers were used to provide both strengthening and toughening mechanisms. The concrete mixture was prepared with fibers representing a High Performance Concrete (HPC). The effect on the mechanical properties of the concrete reinforced with AR glass fibers was studied using various fiber lengths and dosages. The fiber contents of 10 Kg/m^3 and 20 Kg/m^3 were examined. Control specimens without fibers were also prepared for comparison.

Test results indicated that up to 30% cement could be replaced by blended coal flyash, resulting in high strength and ductility. The strength of concrete with 30% flyash was higher than both the control concrete and the concrete containing 20% flyash. At 30% cement replacement, the strength exceeded 7000 psi in the lab, while the field trial

samples exceeded 5000 psi level. The proposed mix design can save up to 40 lbs. of cement per Cu.yd of class P concrete when compared to the mix design of the ADOT.

Test results indicated that there is great potential in reinforcing concrete materials with AR Glass fibers from strengthening and toughening perspectives. The flexure test results indicated that the fiber volume fraction and fiber length have significant effects on the flexural properties of the Fiber Reinforced Concrete (FRC). The concrete with HP12 mm fibers exhibited the optimal flexural strength and toughness with the dosage of 20 Kg/m^3 fibers. The test results also indicated that the increase in fiber length increasing the flexural load capacity with reduction in the toughness. For the hybrid systems, a similar behavior observed was observed with increase in average fiber length increasing flexural load capacity with reduction in the toughness.

To my beloved parents

ACKNOWLEDGEMENTS

I would like to express my sincere thanks and heartfelt gratitude to my advisor and committee chair Dr. Barzin Mobasher for his valuable help and guidance during this period. His expertise, useful ideas and motivation contributed to the success of this research work. I would also like to express my deep thanks and gratitude to Prof. Dr.Alva Peled, Ben-Gurion University, Israel, for her valuable ideas and guidance during this research. Sincere thanks also go to my committee members, Dr. S.D Rajan and Dr. Kamil Kaloush. I owe special thanks to Dr. Dallas Kingsbury for his valuable help with the experimental set-ups.

Finally, a word of appreciation for my family and my friends for their immense support and perennial motivation.

TABLE OF CONTENTS

Page

APPENDIX

LIST OF TABLES

Table Page

LIST OF FIGURES

CHAPTER 1

INTRODUCTION

Two different topics are incorporated in the thesis. The former topic is “The study of concrete with blended coal flyash” and the later is “The study of concrete reinforced with AR Glass Fiber.”

1.1 Flyash Concrete

1.1.1 Background and Objectives

Pozzolanic materials have been successfully used in the past to improve the properties of concrete. The definition for *pozzolans*, based on the ASTM C 618-92a “ Specification for Flyash and Raw or Calcined Natural Pozzolan for Use as a Mineral Admixture in Portland Cement Concrete,” is as follows: “ siliceous or siliceous and aluminous materials, which it self possesses little or no cementitious value but will, in finely divided form and in the presence of moisture, chemically react with calcium hydroxide at ordinary temperatures to form compounds possessing cementitious properties.” Flyash, which is a by-product of coal fired power plants, is currently the most used pozzolan in the construction industry.

Flyash is used in concrete for several reasons including economics, improvements and reduction in temperature rise in fresh concrete, workability, and contribution towards the durability and strength in hardened concrete. Flyash makes efficient use of hydration products in Portland cement. Flyash also helps fill in the spaces between hydrated cement particles in the cement paste fraction of the concrete, thus lowering its permeability. The

lower reaction rate of flyash helps in limiting the amount of early heat generation and the detrimental effect of early temperature rise in massive structures (Neville, 1995).

During the past several years, a large amount of research has been conducted in the area of blended cements with the aim of improving the performance of concrete materials. The mechanical properties of concrete incorporating high volumes of flyash have been studied previously (Carette, Bilodeau, Chevrier, & Malhotra, 1993). Cement in the concrete was replaced with flyash up to 55 % to 60% and the properties of fresh and hardened concrete were investigated. This study concluded that a high performance air – entrained high volume flyash concrete could be produced. The results from this study indicated low creep and low drying shrinkage along with excellent mechanical properties at both early and late ages for the concrete mixture. There have been reports in the literature citing the use of high volume class C and class F flyash in the pavement construction (Naik, Ramme, & Tews, 1995). Results of this particular study indicated excellent mechanical properties for the class F flyash mixture compared to the conventional cement mixtures used for paving concrete.

These research efforts point out the beneficial aspects of using flyash by improving the performance of concrete materials. There are several short term and long term cost savings associated with the use of flyash. In addition, the combination of mineral admixtures such as flyash, silica fume, and superplasticizer with careful selection of constituent materials has made the production of High Performance Concrete (HPC) easier and more economical.

A significant amount of research work has been conducted at Arizona State University in the area of blended cements with the aim of improving the performance of concrete materials. The cement and concrete materials research group of ASU has developed theoretical and experimental methodologies in the analysis of blended cements and high performance concrete materials. Several manuscripts have been published in this area and the effect of flyash on the strength, durability, chemical and pozzolanic reaction, porosity, hydration, etc. has been documented (Tixier & Mobasher, 2000).

The properties of concrete are dependent on several factors including the degree of hydration, water cement ratio, porosity, age, and curing conditions. An experimental program on the influence of flyash level and various activators on the strength, fracture, tension, and shrinkage properties of high-performance concrete is conducted. The micro structural and mineralogical effects of flyash on the strengthening and toughening mechanisms of concrete are studied. One of the main objectives of this study is the specification aspect of the use of flyash.

Under the present guidelines of Arizona Department of Transportation, (ADOT) use of flyash up to 20% as a partial replacement of cement in concrete is permitted. One of the objectives here is to study the effect of increasing the volume of flyash to 25% and 30% and implement the developed mix designs into the field trials. The main aim is to develop mixes, which conform to the class P concrete mix for highway applications as, used by ADOT, and showcase the work through field trials. In order to achieve this task, various mechanical properties of several mixtures of flyash concrete were studied.

Finally, the results were compared with the current mix design procedures used as the control mix design.

1.1.2 *Research Methodology*

The proposed method of approach is to develop mix designs in the laboratory, which meet the specification requirements with comparable cement contents, and strengths of mixtures currently used for class P concrete. The next step is the measurement of mechanical properties of these mixtures. Finally these mixtures will be implemented in a field trial.

It is well known that flyash results in low early age strength. Therefore in addition to compressive strength tests, three-point bending tests were also conducted. The mixtures were evaluated by their strength development at 7 days and 28 days. The strengthening and toughening mechanisms of flyash cement concrete under compression, and normal flexure studied. The studies conducted previously were based on high cement content. These studies were used as the basis for comparison of the current mix formulations.

1.2 Concrete with AR Glass Fibers

1.2.1 Background and Objectives

Reinforcing ordinary concrete materials with glass fibers has been attempted for more than 20 years (Frondistouyannas, 1977; Shah & Mobasher, 1989). Use of Alkali Resistant (AR) glass fibers in concrete presents an area of opportunity to utilize the strength and stiffness of fibers in reinforcing the brittle matrix. Concrete materials produced with short randomly distributed AR Glass fibers would be superior to other

FRC (Fiber Reinforced Concrete) materials for several reasons. It has been shown that due to the reduced specific spacing, fibers strengthen the composite at the micro level by bridging the microcracks before they reach the critical flaw size (Mobasher & Li, 1996). In comparison to steel fibers, the small diameter of the individual glass fibers ensures a better and more uniform dispersion. In addition, the high surface area and relatively small size of glass fiber bundles offers significant distribution capability and crack bridging potential as compared to steel fibers. The glass fibers are randomly distributed offering efficiency in load transfer. Furthermore, the bond strength of the glass fiber is far superior to the polypropylene fibers, thus increasing the efficiency of fiber length so that there is limited debonding and fiber pullout. Finally, due to the highly compliant nature of the glass fiber bundles which bridge the matrix cracks at a random orientation, they are able to orient so as to carry the load across the crack faces.

1.1.2 *Research Methodology*

In the Fiber Reinforced Concrete (FRC) study, two types of AR Glass fibers were examined 1) High dispersion (HD) and 2) High Performance (HP) to provide both strengthening and toughening mechanisms. Various fiber lengths and contents were studied for both fiber types. The concrete mixture was prepared with the fibers representing a HPC (High Performance Concrete) mixture. Control specimens without fibers were also prepared for comparison. The fiber contents of 10 kg/m^3 and 20 kg/m^3 were used.

1.3 *Organization of the Thesis*

Chapter 1 provides the introduction and research methodology for concrete with blended coal flyash and concrete reinforced with AR Glass fibers. Chapter 2 provides the experimental program including development of the mix design for high dosage of flyash in concrete and experimental procedure and results for flexure and compression tests conducted in the laboratory.

Chapter 3 provides the implementation of the mix design developed for the high dosage of flyash in concrete in the lab into the field in collaboration with ADOT. It also includes experimental testing and results of the samples collected from the field trial.

Chapter 4 provides the experimental program to study the mechanical properties of AR Glass fibers in the concrete. It includes specimen preparation and experimental results of flexure and compression test conducted to study the effects of fiber types, fiber lengths, fiber contents and hybrid system of fibers containing various lengths of fibers in the FRC.

Chapter 5 summarizes the work presented in this thesis, and provides the conclusion.

CHAPTER 2

EXPERIMENTAL PROCEDURE AND RESULTS FOR FLYASH CONCRETE

2.1 Introduction

This chapter discusses the test mixes, specimen characteristics and Experimental study conducted to evaluate the mechanical properties of concrete containing blended coal flyash. The influence of blended coal flyash on concrete mixes was studied. To increase the use of flyash in concrete from 20% to 30%, a standard mix design procedure was developed and various samples were tested for compression and flexural strength. Concrete specimens containing class F flyash and superplasticizer were prepared. Concrete with 30-35% flyash was prepared with both high and low superplasticizer content. Two different water-binder ratios of 0.42 and 0.45 were used. Two categories of concrete mixtures were developed. Three replicate samples from each batch were tested at 7 and 28 days. Effects of age, water cement ratio and superplasticizer on compression and flexural strengths were studied. To achieve the above goal both closed-loop compression and flexural (Three point bending) tests were conducted.

2.2 Development of Mix Designs

A concrete mix having a characteristic compressive strength (f_c') of 4000 psi and a slump of 2-2.5" was developed. To achieve the above task two categories of concrete mixtures were developed. In the first category, the high proportion of cement and flyash were used to accentuate the effect of flyash on the mechanical properties. These are identified as GROUP I set of mixtures, and reflect the effect of flyash on the properties of concrete. These mixtures were

developed previously in the ASU laboratory and presented here to compare with Low Cement mixtures only.

The second category of the mixtures was developed considering the economical and commercially realistic mix designs with flyash, which met the specifications for use in highway applications. These mixtures were developed according to class P concrete mix design and were compared with current mix design procedures of ADOT. Concrete with 30% and 35% flyash was prepared with both high and low superplasticizer content. The superplasticizer was used at a dosage of 200 ml per 100 kg of total cementitious materials for low dosage and 400 ml per 100 kg of total cementitious materials for high dosage. Two different water-binder ratios of 0.42 and 0.45 were used. Effects of water cement ratio and superplasticizer were studied to make sure that the developed mixes met both the strength and workability criteria. These are identified as GROUP II set of mixtures. Table 2.1 and 2.2 present the mix design with both high and low cements contents, which were used in current and past experiments.

2.3 Specimen Preparation

All materials preparation, proportioning, mixing and testing in the laboratory were in accordance with the ASTM C39 and C109 standards. Slump of fresh concrete was determined according to ASTM C143. Concrete mixtures were cast using a vibration table to help with the consolidation of the fresh mixture in the molds. All the specimens were filled in two layers with proper consolidation in between layers. From each mix, the following specimens were made:

1) Flexure Test - 4 replicate samples of $457.2 \times 101.6 \times 101.6$ mm (18x 4x 4 in.)
2) Compression Test - 3 replicate samples of 152.4 x 76.2 mm (3 x 6 in.)

In order to achieve a desired slump and cohesive concrete mix, the following mixing procedure was adopted. The dry coarse aggregate and sand were introduced in the mixer and blended for 90 seconds with superplasticizer and half of the mixing water. Then, cement, flyash and remaining water added to the mixer and blended for 3 additional minutes to thoroughly mix all the ingredients. All the specimens were filled in two layers with proper compaction in between the layers. A vibration table was used to help with the consolidation of the fresh mixture in the molds. After 24 hrs, specimens were placed in a curing room at 90% (RH) and 23^0 C (70^0 F) for 7 and 28 days curing. A water-cooled diamond blade circular saw was used to cut a 12.7 mm (0.5 in.) notch at the mid-span of the specimens for three point bending flexure tests. The specimens were allowed to dry in the laboratory for 12 hrs prior to the tests.

2.4 Test Procedure and Results

2.4.1 Compression Test

The compression test is perhaps the most common tool used for characterizing concrete mixtures. This test is conventionally used to obtain the ultimate strength and the modulus of elasticity. In the present study, the test is extended to obtain the entire stress-strain response of the specimen including the post-peak region. Figure 2.1 shows the schematics of the instrumented specimen used to obtain the complete stress strain response. Compression tests were conducted using a 110 Kips SBEL testing machine operated under closed-loop control. A special ring type fixture was developed to attach two LVDT's to measure the axial strain in the specimen. A gage length of 2.5" was used to measure the axial strain. This axial displacement measuring fixtures was attached to the specimen using spring plungers that allowed the LVDT's

to move as the specimen deformed in the direction of load. This fixture also permitted the deformations to be measured as the specimen underwent the post peak response. A chain type fixture was placed around the specimen to which an extensometer was attached. The extensometer measures the circumferential strain.

The standard ASTM tests are conducted under load control or actuator displacement control. In the above cases, once the maximum load is reached, the resistance of the specimen to carry an increasing load level is exhausted. If the test is not controlled to adjust the load applied, the specimen shatters under the increasing load. The net result obtained from this test is the compressive strength only. The test configuration needed for obtaining the stable post-peak response in compression test depends on the behavioral class and the brittleness of the material. Several options are available for a controlled variable including load, stroke, axial displacement, circumferential displacement, and their combinations.

The post-peak response was obtained using circumferential displacement as the controlled variable. The test initially started under load control, and prior to the peak load, the control was transferred to the circumferential displacement by using extensometer. Using combination of these two control parameters, it was possible to capture the post-peak response. The circumferential deformation always increases throughout the test, however, its increase may not be sensitive to the loading during the prepeak regime. Initially using load as the controlled variable and then switching to circumferential deformation as the control when the specimen begins to dilate significantly overcome the problem. The test could be lost if the damage or failure plane localize within a zone that is completely outside the plane being monitored by the

extensometer. This problem is not common but could occur in slender specimens or especially very weak concrete that crush near the loaded faces. The response of the specimen viewed in the context of initial linear response in the stress strain curve, followed by a non-linear response due to the microcrack evolution in the samples leading to the ultimate strength. Beyond ultimate strength, the load is decreased as the strain is increased. This is attributed to the formation of major cracks and progressive damage in the specimen and is referred to as the post peak response. The post peak response clearly demonstrates the behavior of specimen in terms of its ductility and energy absorption capacity.

2.4.2 Compression Test Results

It is well known that the partial replacement of cement by flyash may result in lower compressive strength at early ages. This is expected to be followed by the development of greater strength at later stages. The results of the compressive strength for all the mixtures in the group I series are presented in Table 2.3. It indicates that the average 28 days compressive strength of 4181, 4630, 5808, and 6788 are obtained for 0, 20, 25, 30% flyash content respectively. It is noted that the strength of concrete with 30% flyash is higher than both control concrete and concrete with 20% flyash. Figure 2.2 presents the increased compressive strength with the use of flyash. Note that with 30% cement replacement the strength exceeds 7000 psi.

Figure 2.3 presents the effect of flyash content on the compression strength of concrete for samples of group II series at 7 days testing. These specimens have significantly lower cement content than the group I series of mixtures. The sensitivity of the results with respect to water cement ratio and superplasticizer content in this range is not apparent, indicating a more or less

similar response within the range studied. The average compressive strength of the mixtures in this series is in the range of 2186 to 2330 psi for water cement ratios of 0.42 to 0.45 at 7 days testing. The strength of these mixtures reaches levels of 3901 to 3728 psi for the same levels of water cement ratios at 28 days.

Figure 2.4 presents the compression test result at 28 days. From the graph it can be noticed that the concrete with 30% flyash has higher compressive strength than the concrete with 35% flyash with low superplasticizer content. The average compressive strength of concrete with 30% flyash at 28 days is 4125 psi, which is about 10% more than the concrete with 35% flyash content at 3701 psi. Figure 2.5 and figure 2.6 present the effect of superplasticizer content and water cement ratio on the compressive strength respectively. It can be noticed that the superplasticizer has no significant effect on strength except on rheology of concrete. While the effect of superplasticizer is not apparent, there is a marked increase in the compressive strength with reduction of water cement ratio from 0.45 to 0.42. This also indicates that the 30% is the maximum allowable level of use of flyash for the concrete, if we need to maintain the 4000psi strength at 28 days. Test results are tabulated in Tables 2.4 and 2.5.

Figure 2.7 represents the effect of age on compressive strength for a typical specimen. Note that from 7 to 28 days there is a significant increase in the compressive strength. Figure 2.8 shows the effect of cement content on the compressive strength. Note that the higher cement content will obviously increase the compressive strength from 4000 to 7000 psi at 28 days.

Based on the 7 and 28 days test results, from the strength point view, there should be no problem using concrete with levels higher than the current 20% flyash up to 30%. Concrete with

30% flyash gives the optimum results for the compressive strength of a mix design for class P concrete; hence, this level was suggested for the development of field trials.

2.4.3 Flexure Test

The behavior of the specimen under flexure is dominated by the cracking that initiates at the notch and grows along the depth of the specimen. As such a test progresses, the deformation localizes at the notch and is followed by crack propagation. Since the critical deformations are the opening of the crack tip that may be measured at the base of the notch, the best-controlled variable in flexure tests is the crack mouth opening or a similar displacement. The deflection of the specimen is also measured to compute the energy absorbed throughout the test.

Flexure tests may be conducted under several loading configurations. Since the tensile strength of concrete is relatively low, the tests involved with only opening or tensile displacements along the crack are called mode I tests and are quite important. The most popular mode I test configuration for concrete is the notched beam loaded at mid-span. The test is performed under Closed Loop Control with crack mouth opening deformation (CMOD) as the controlled variable. Figure 2.9 presents the flexural test setup. In this test, the crack mouth opening displacement (CMOD) was measured across the face of notch using an extensometer. Three point bend flexural tests were performed on 18” x 4” x 4” beam specimens with an initial notch of 0.5”. A test span of 16” was used. The deflection of the beam was also measured using a spring-loaded linear variable differential transformer (LVDT) with a 2.54 mm (0.1 in) range. A displacement measuring yoke was developed to measure the centerline deflection of the beam

with respect to the supports. This device eliminates extraneous deformations such as support settlements and specimen rotations.

2.4.4 Flexure Test Results

Analysis of the flexural test results was conducted to evaluate the influence of flyash on the flexural properties. A comparison of flexural response of concrete with various levels of flyash was conducted and reported in an earlier study (S. A. Mane, R. Tixier, & B. Mobasher, 2001). The present study only focuses on the response of concrete with 30% flyash as affected by various amounts of superplasticizer and water cement ratio. Figure 2.10 represents the load vs. deflection response for a series of specimens made with several levels of flyash ranging from 30-35%. In the pre-peak region all curves behave in similar manner. In the post peak region, the specimen with 30% flyash and a w/binder ratio of 0.42 shows the highest amount of energy absorption.

Figure 2.11 presents the load vs. deflection curve for 30 and 35% flyash in concrete with different superplasticizer content at 28 days. From the above graphs it can be observed that the there is not much difference in strength of concrete with 30% flyash and the concrete with 35% flyash with difference in strength less than 5% only. The nominal load at failure is measured around 973 lbs at 7 days and 1135 lbs at 28 days cured specimens. This results in average flexural strength of about 317 psi and 370 psi respectively. The post peak response in concrete with 35% flyash is comparable or better than 30% flyash concrete in terms of ductility and energy absorption capacity. The average energy absorption of these series of mixes increases

from 6.45 to 10.56 lbs. in from 7 to 28 days. It is also observed that the superplasticizer has a minor effect on the flexure strength of the concrete.

Figure 2.12 represents the effect of age on the flexural response of both high and low cement content mixtures. Note that both the age and cement content affect the flexural strength in a proportional manner. Figure 2.13 presents that superplasticizer has marginal effect on flexural Strength, while the effect of water cement ratio on the flexural strength is substantial as shown Figure 2.14.

Table 2.1

Summary of Mix Designs

Mix ID	Cement Content	% FA Content	W/C	Superplasticizer Content
Group I				
H_40_LS	High	0	0.40	Low[1]
H20_40_LS	High	20	0.40	Low
H25_40_LS	High	25	0.40	Low
H30_40_LS	High	30	0.40	Low
Group II				
L30_42_HS	Low	30	0.42	High[2]
L30_42_LS	Low	30	0.42	Low
L35_42_LS	Low	35	0.42	Low
L30_45_HS	Low	30	0.45	High
L30_45_LS	Low	30	0.45	Low

1) Low: 200ml/100 kg of cementious materials

2) High: 400ml/100 kg of cementious materials

Table 2.2

Mix Design for Group I- (High Cement Content) and Group II- (Economical Cement Content)

Mix ID #	% FA	Cement Content	Flyash Content	W/B	Dry weight of materials, Kg				
		lbs/Cu.yd	lbs/Cu.yd		Cement	Flyash	Water	FA	CA
Group I									
H_40_LS	0	1129	-	0.40	8.68	-	3.47	7.5	9.86
H20_40_LS	20	941	188.75	0.40	7.23	1.45	3.47	7.5	9.86
H25_40_LS	25	903	226.50	0.40	6.94	1.74	3.47	7.5	9.86
H30_40_LS	30	868	260.34	0.40	6.67	2.00	3.47	7.5	9.86
Group II									
L30_42_LS	30	493	148	0.42	4.83	1.45	2.64	12.5	16.41
L30_42_HS	30	493	148	0.42	4.83	1.45	2.64	12.5	16.41
L35_42_LS	35	480	158	0.42	4.61	1.61	2.64	12.5	16.41
L30_45_LS	30	490	147	0.45	4.80	1.44	2.81	12.3	16.17
L30_45_HS	30	490	147	0.45	4.80	1.44	2.81	12.3	16.17

Table 2.3

Compression Test Results for Group I Series of Mixes (28 days)

Mix ID #	Fly ash (%)	Strength (psi)	Strain at peak Load, (in/in)		Modulus of Elasticity (psi)	Poisson's Ratio	Toughness, (lbs. in)
			Axial	Lateral	Axial		
			10^{-3}	10^{-4}	10^{6}		
H_40_LS_1	0	3727	2.009	101	3.34	0.122	61.75
H_40_LS_2	0	4635	0.645	141	8.51	0.201	54.6
H20_40_LS_1	20	4630	1.308	45.70	5.12	0.20	80
H25_40_LS_1	25	5808	2.220	3.78	3.91	0.106	43.2
H30_40_LS_1	30	7461	2.441	-	4.07	-	-
H30_40_LS_2	30	6115	1.058	1.02	3.79	0.16	51.58

Table 2.4

Compression Test Results for Group II Series of Mixes (7 days)

MIX ID #	W/C	Strength	Avg. Strength (Std Dev)	Strain at Peak Load, (in/in)		Modulus of Elasticity psi	Poisson's Ratio
		psi	psi	Axial 1.0E-03	Lateral 1.0E-03	Axial 1.0E+06	
L30_42_HS_1	0.42	2136	2255 (169)	8.42	1.365	3.81	0.22
L30_42_HS_2	0.42	2375		7.49	1.00	5.68	0.2
L30_42_LS_1	0.42	2129	2184 (77.78)	-	1.45		-
L30_42_LS_2	0.42	2239		8.7	1.1	6.86	0.3
L35_42_LS_1	0.42	2055	2055	9.15	0.92	5.24	0.24
L30_45_HS_1	0.45	2220	2354 (189.5)	4.75	1.39	4.58	0.18
L30_45_HS_2	0.45	2488		5.03	1.46	4.79	0.24
L30_45_LS_1	0.45	2529	2315 (187.1)	5.36	3.42	4.87	0.27
L30_45_LS_2	0.45	2234		2.69	1.26	2.34	0.2
L30_45_LS_3	0.45	2182		4.67	0.94	4.58	0.22

Table 2.5

Compression Test Results for Group II Series mixtures (28 days)

MIX ID #	W/C	Strength	Avg. Strength (Std. Dev)	Strain at Peak Load, (in/in)		Modulus of Elasticity psi	Poisson's Ratio
		psi	psi	Axial	Lateral	Axial	
				1.0E-3	1.0E-3	1.0E+07	
L30_42_HS_1	0.42	3850	3850	1.245	3.578	3.35	0.19
L30_42_LS_1	0.42	4242	4127.5 (161.9)	5.21	1.414	7.31	0.3
L30_42_LS_2	0.42	4013		3.73	1.091	4.21	0.35
L35_42_LS_1	0.42	3674	3701.5 (38.89)	6.17	4.47	4.32	0.2
L35_42_LS_2	0.42	3729		8.41	6.81	2.91	0.21
L30_45_HS_1	0.45	3716	3698.5 (24.75)	18.4	16.92	1.55	0.21
L30_45_HS_2	0.45	3681		17.5	14.4	2.84	0.16
L30_45_LS_1	0.45	3842	3749 (86.85)	12.1	1.503	4.84	0.22
L30_45_LS_2	0.45	3735		7.69	0.65	3.65	0.14
L30_45_LS_3	0.45	3670		7.64	0.73	4.54	0.18

Table 2.6

Three Point Bending Test Results (7 days)

Mix ID	W/C	% FA	At the Peak							Toughness	Avg Toughness
			Load	Avg Load	Effective Strength	CMOD in	Avg CMOD in	Deflection	Avg Deflection in		
			lbs	lbs	psi	1.0E-03	1.0E-03	1.0E-03	1.0E-03	lbs.in	lbs.in
L30_42_HS_1	0.42	30	967	982.5 (21.92)	320.82	1.594	1.335	1.528	1.393	6.1	7.35
L30_42_HS_2	0.42	30	998			1.077		1.258		8.6	
L30_42_LS_1	0.42	30	1010	993 (24.74)	324	1.694	1.403	1.774	1.509	8.9	7.55
L30_42_LS_2	0.42	30	975			1.112		1.245		6.2	
L35_42_LS_1	0.42	35	967	967	315.76	1.306	1.306	2.105	2.105	6.8	6.8
L30_45_HS_1	0.45	30	972	954 (26.2)	311.25	1.22	0.99	1.154	1.007	5.9	4.85
L30_45_HS_2	0.45	30	935			0.76		0.86		3.8	
L30_45_LS_1	0.45	30	948	969 (29.7)	316.41	1.072	1.153	-	1.557	-	5.7
L30_45_LS_2	0.45	30	990			1.235		1.557		5.7	

Table 2.7

Three Point Bending Test Results (28 days)

Mix ID	W/C	% FA	At the Peak							Toughness	Avg. Toughness
			Load	Avg Load	Effective Strength	CMOD in	Avg CMOD in	Deflection in	Avg Deflection in		
			lbs	lbs	psi	1.0E-03	1.0E-03	1.0E-03	1.0E-03	lbs.in	lbs.in
L30_42_HS_1	0.42	30	1078	1103 (35.36)	360.16	1.872	1.9515	1.854	1.854	10.1	10.1
L30_42_HS_2	0.42	30	1128			2.031		-		-	
L30_42_LS_1	0.42	30	1182	1151 (43.8)	375.84	1.075	1.173	1.935	2.233	15	14
L30_42_LS_2	0.42	30	1120			1.271		2.531		13	
L35_42_LS_1	0.42	35	1280	1210 (99)	395.1	1.271	1.236	2.531	2.105	10.8	11.6
L35_42_LS_2	0.42	35	1140			1.201		2.619	2.105	12.4	
L30_45_HS_1	0.45	30	1159	1100 (83.4)	359.2	0.614	0.9385	1.923	1.7155	7.2	7.7
L30_45_HS_2	0.45	30	1041			1.263		1.508		8.25	
L30_45_LS_1	0.45	30	1054	1112 (82.0)	363.1	1.416	1.835	1.881	1.9475	10.9	9.4
L30_45_LS_2	0.45	30	1170			2.254		2.014		7.85	

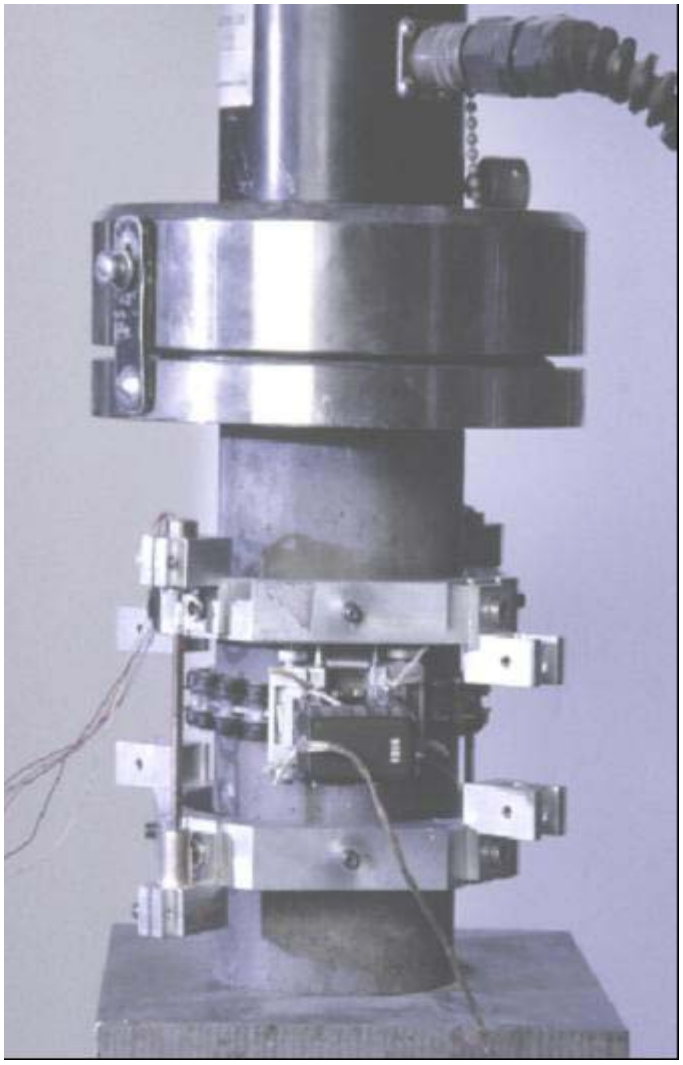

Figure 2.1. The closed-loop compression test set up

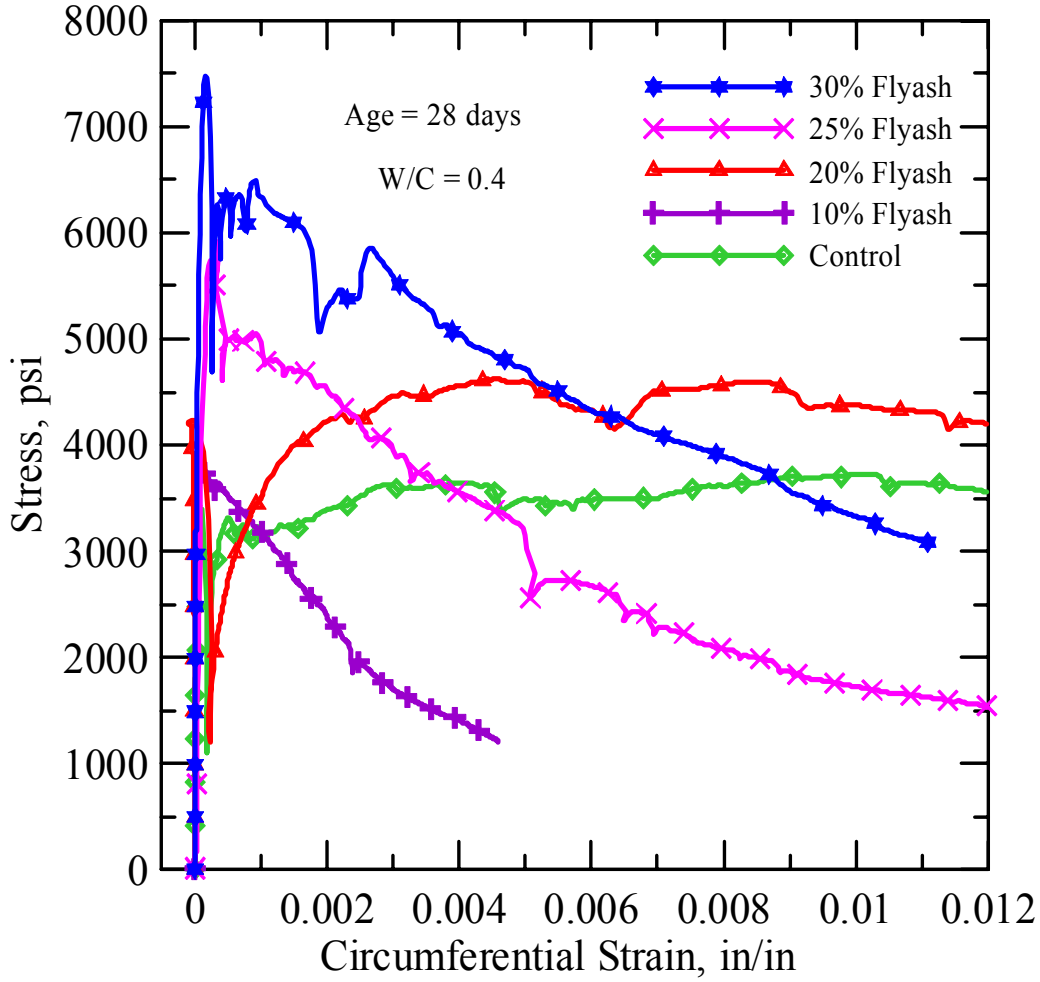

Figure 2.2. Stress vs. Circumferential Strain at 28 days with various flyash contents and high cement contents

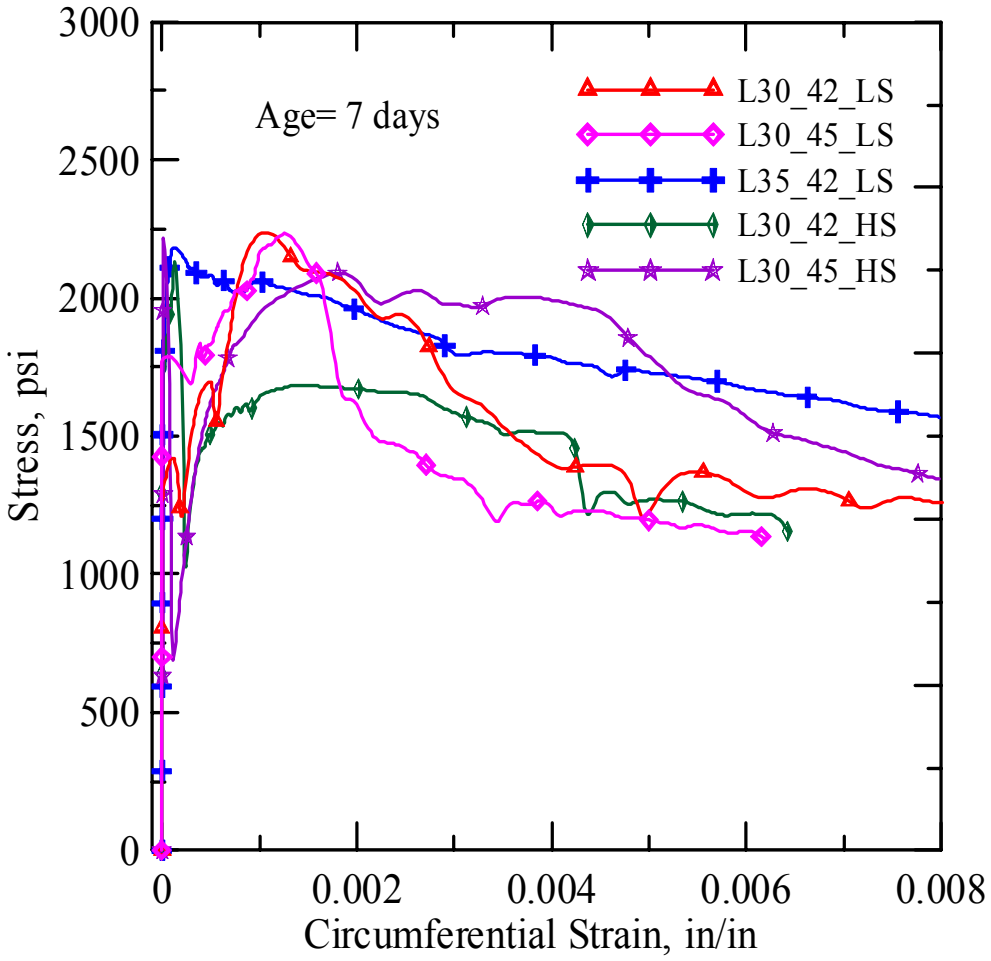

Figure 2.3. Stress vs. Circumferential Strain for 30 & 35% flyash at 7 days of curing (Group II)

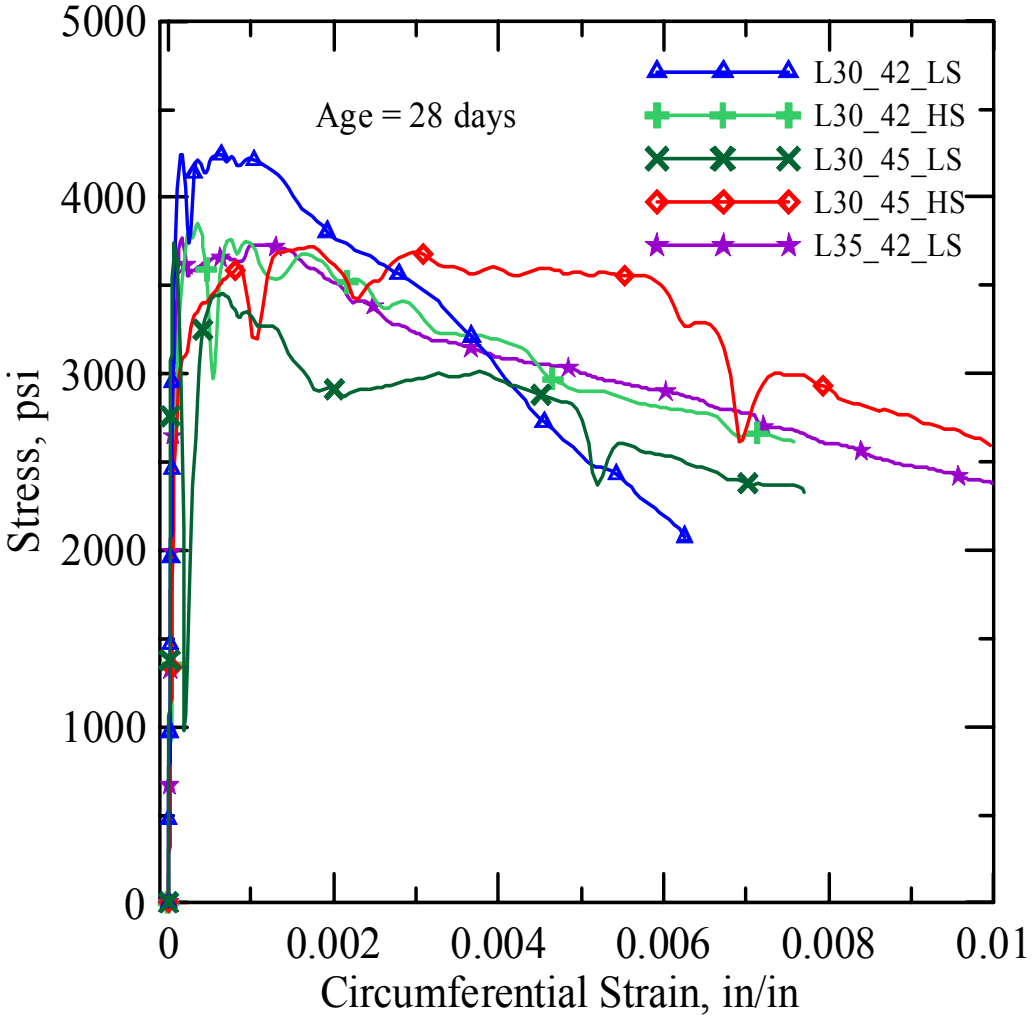

Figure 2.4. Stress vs. Circumferential Strain for 30 & 35% flyash at 28 days of curing (Group II)

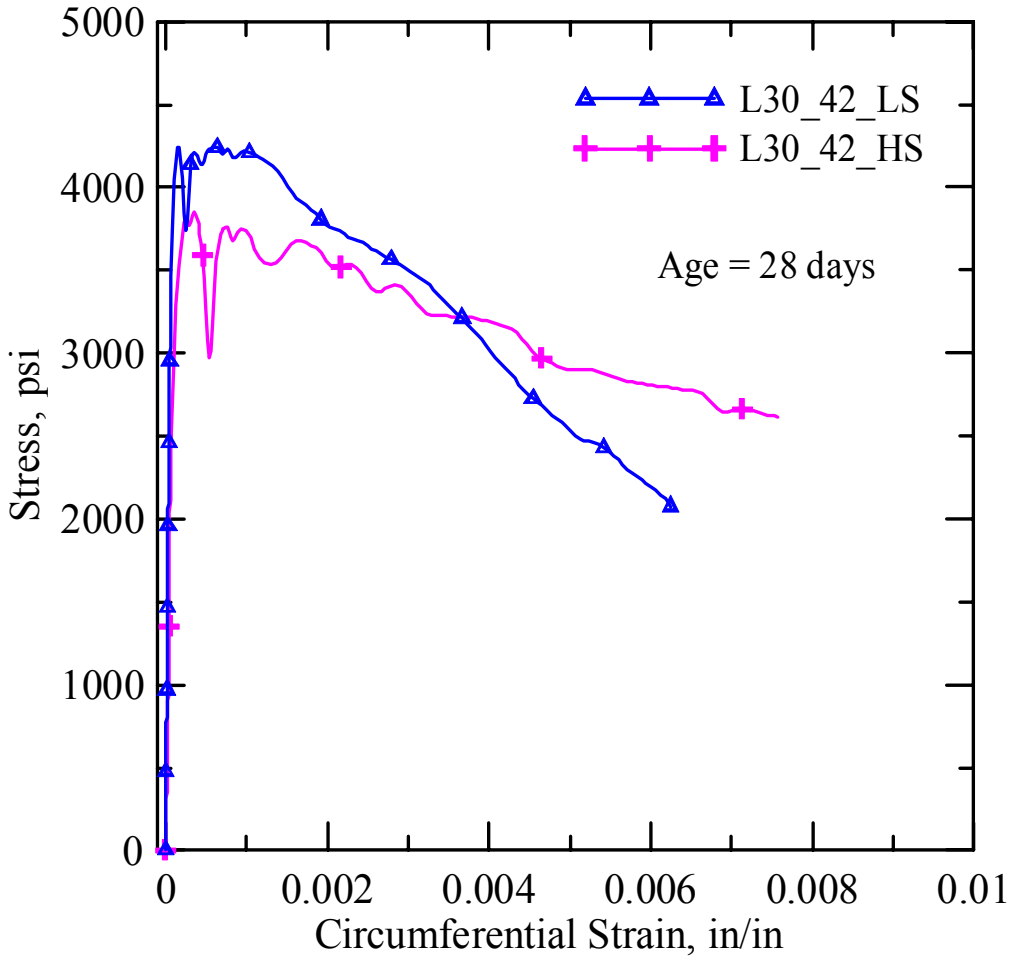

Figure 2.5. Effect of superplasticizer on the compressive strength

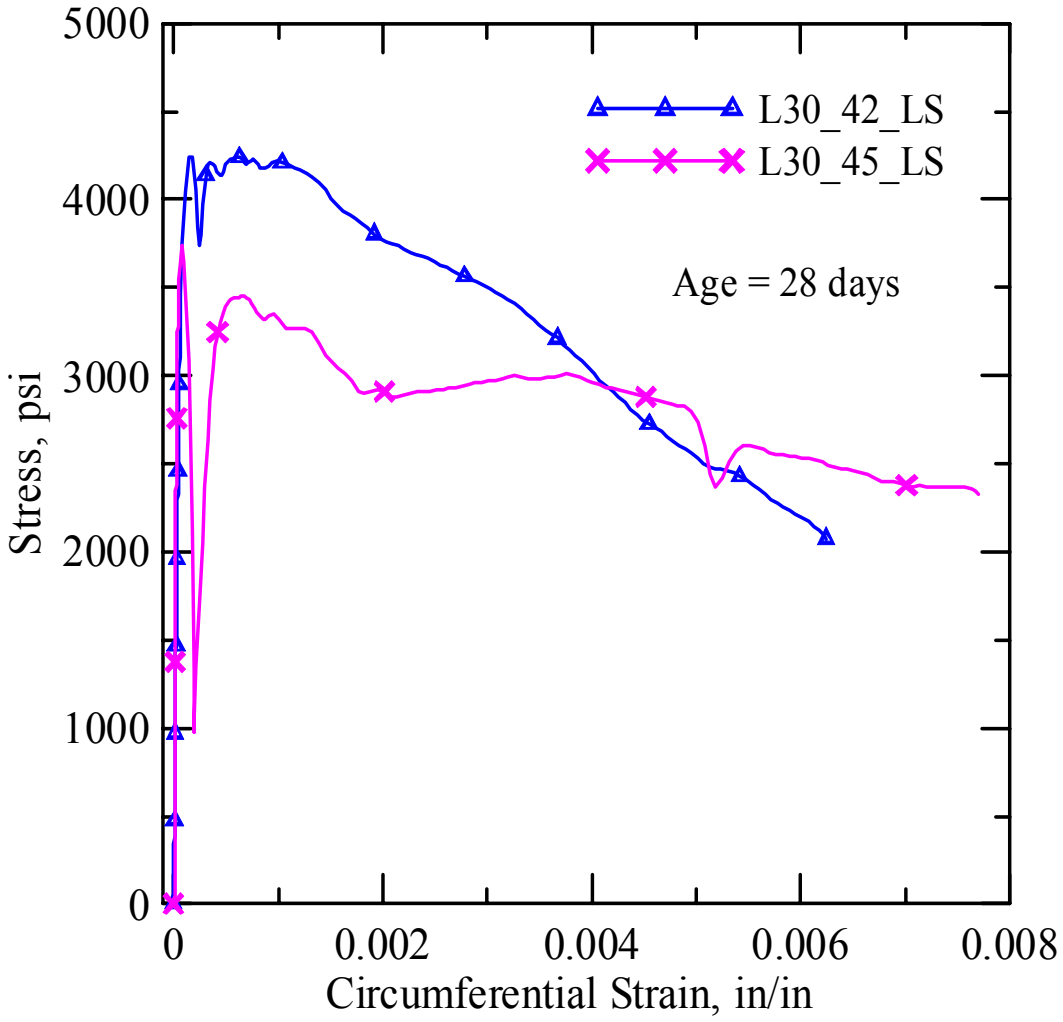

Figure 2.6. Effect of water cement ratio on the Compressive strength

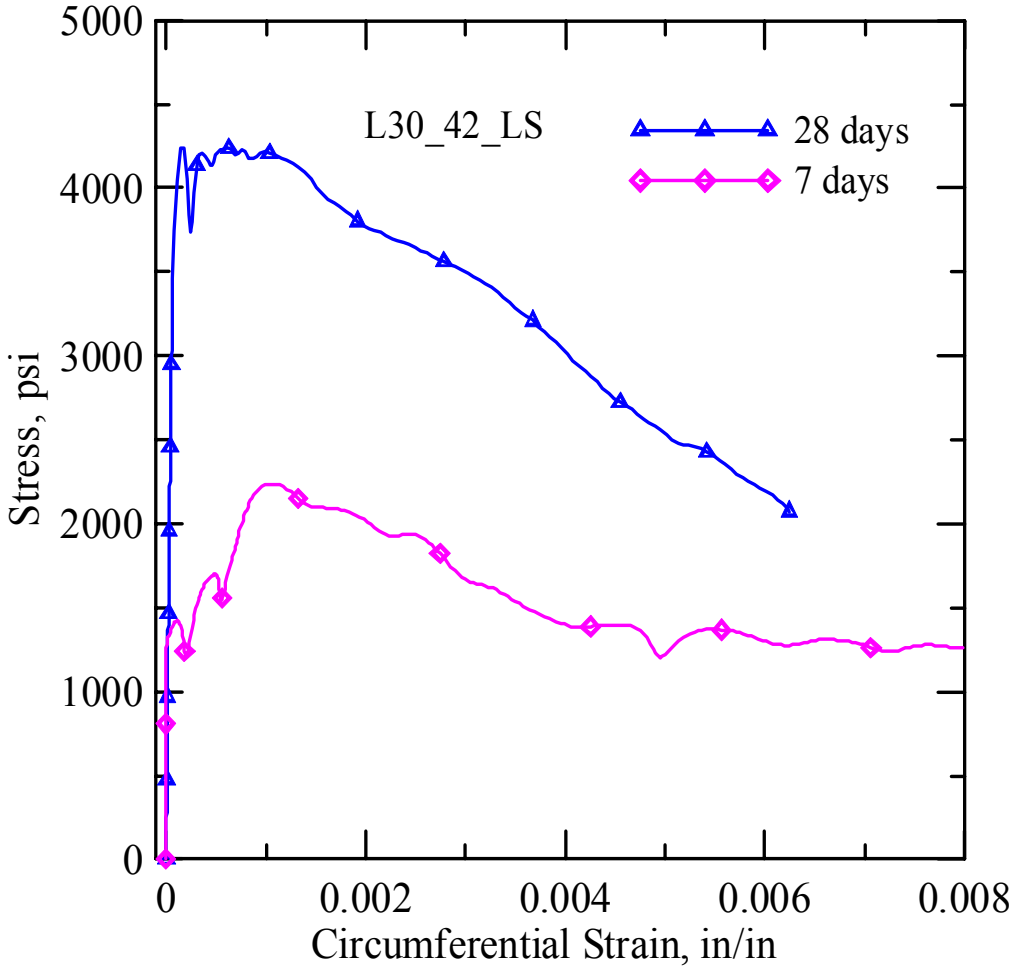

Figure 2.7. Effect of age on the compressive strength

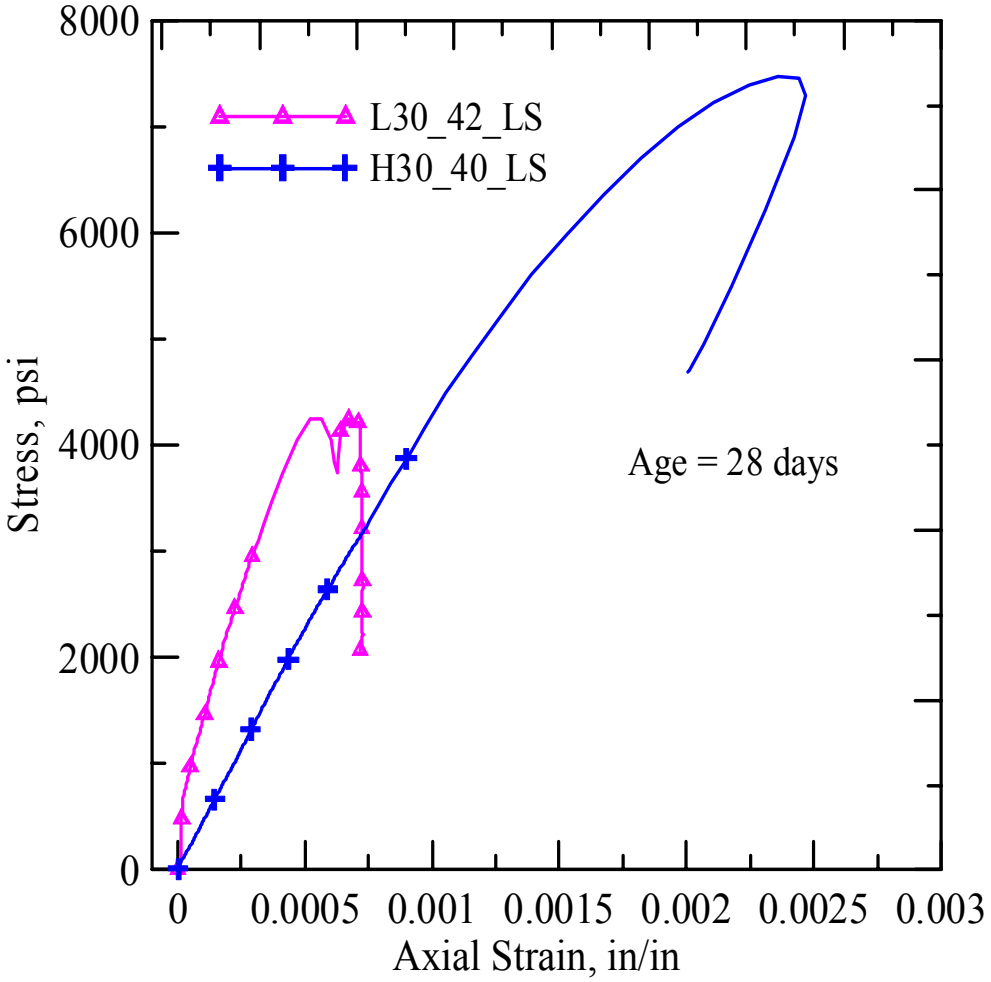

Figure 2.8. Effect of cement content on the compressive strength

Figure 2.9. The closed-loop flexural test set up

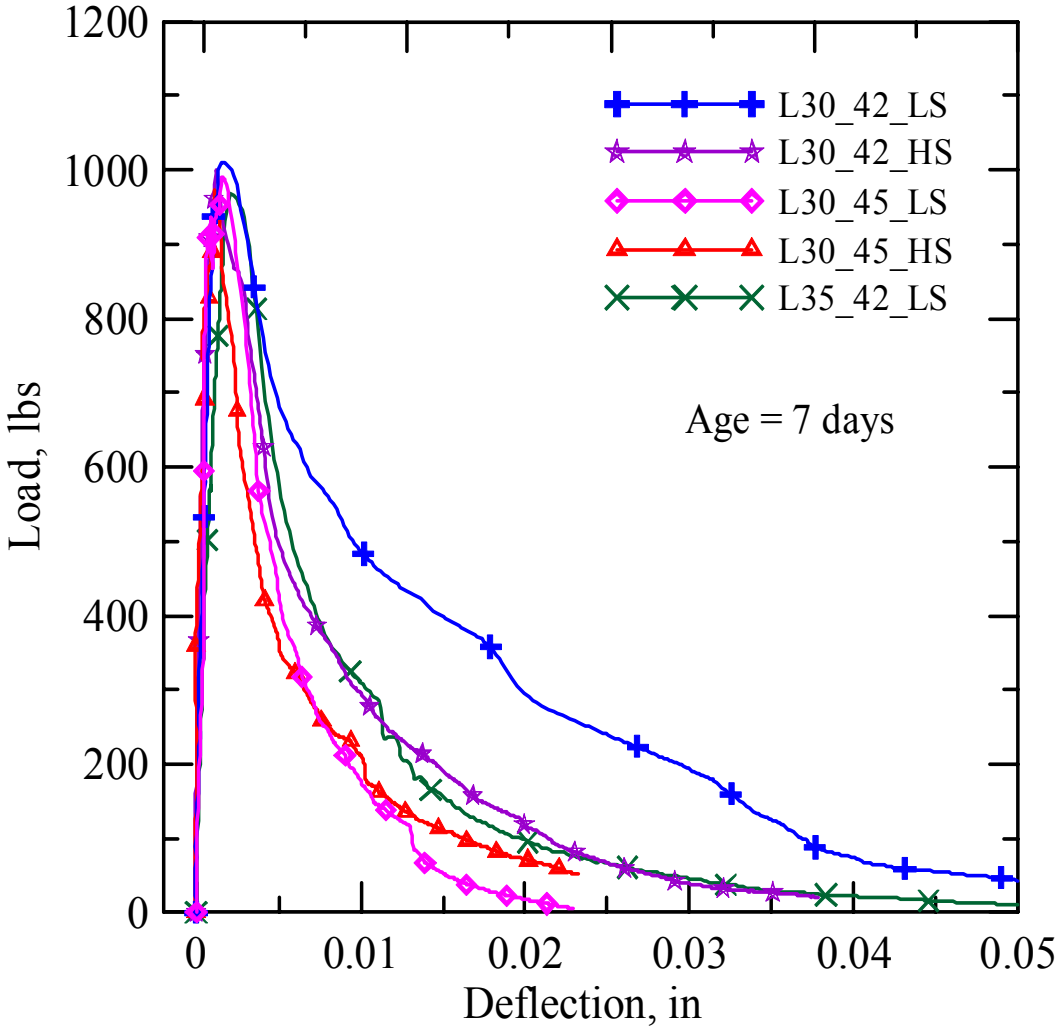

Figure 2.10. Load vs. Deflection for 30% and 35% flyash in concrete with different superplasticizer content (7 days)

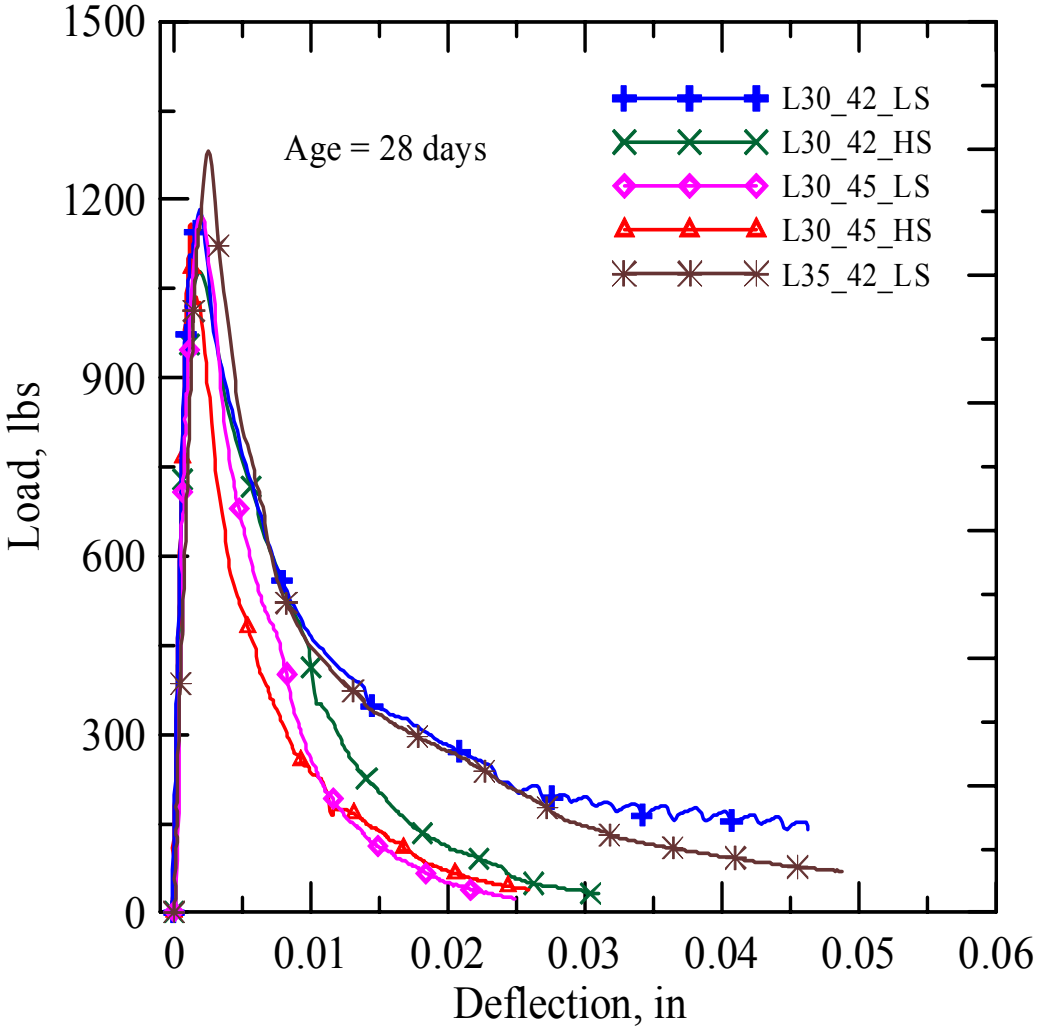

Figure 2.11. Load vs. Deflection for 30% and 35% flyash in concrete with different superplasticizer content (28 days)

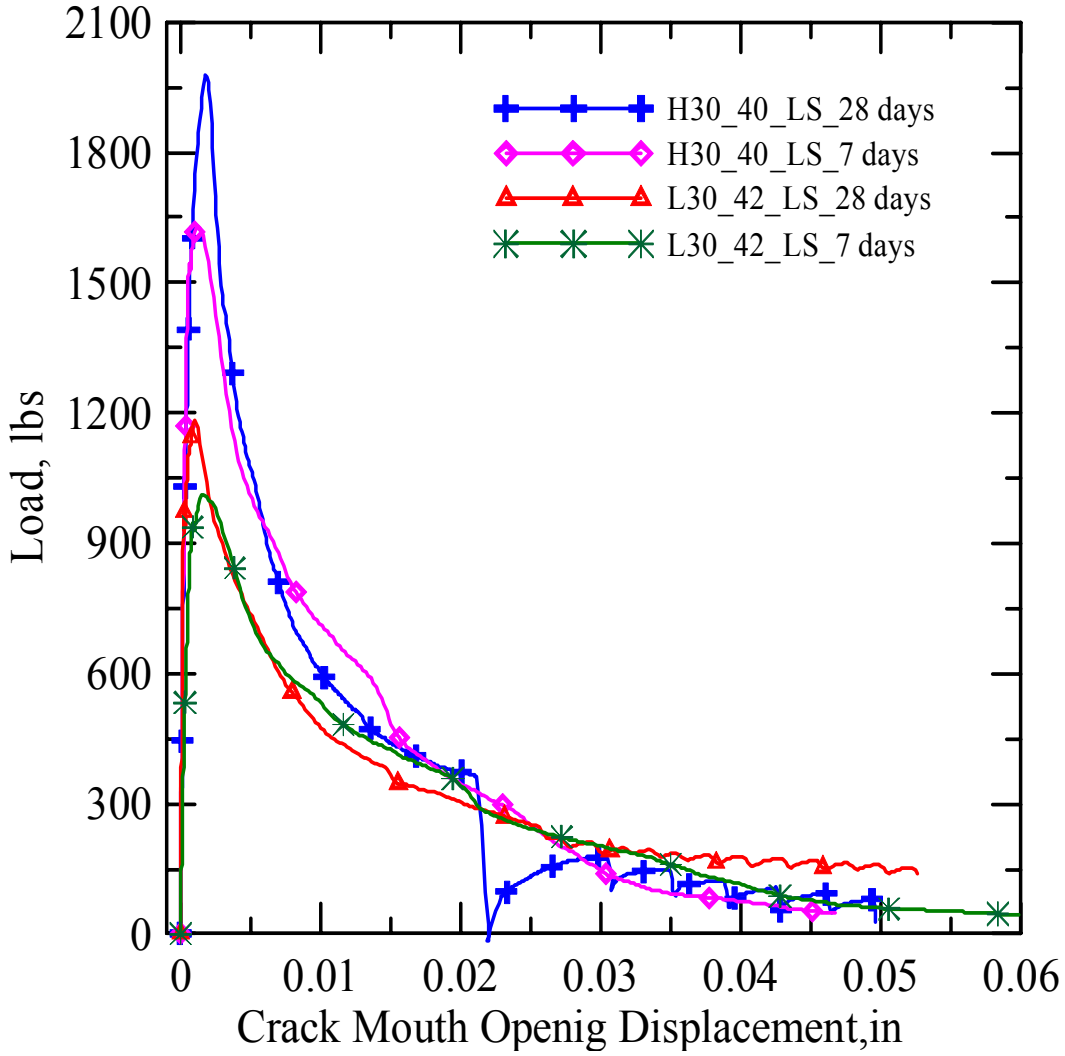

Figure 2.12. Effect of age on the flexural Strength

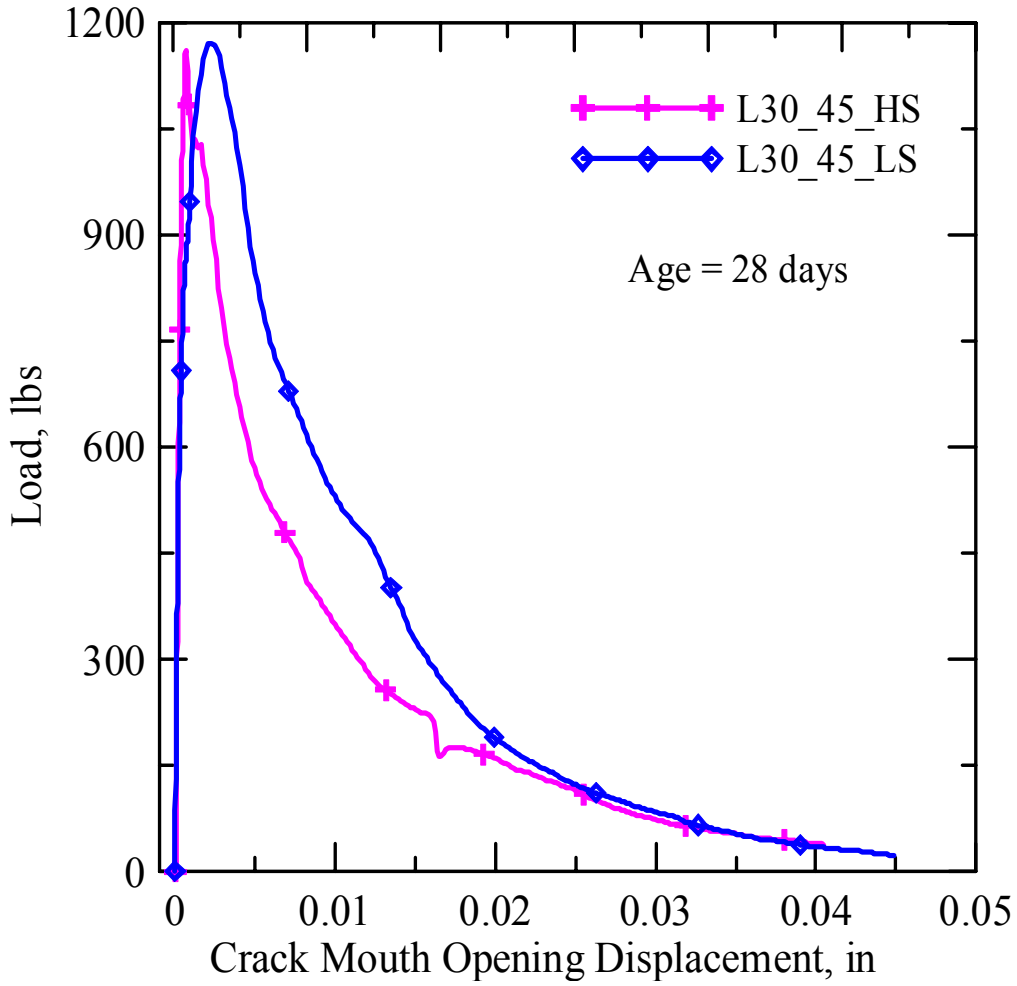

Figure 2.13. Effect of superplasticizer on the flexural Strength

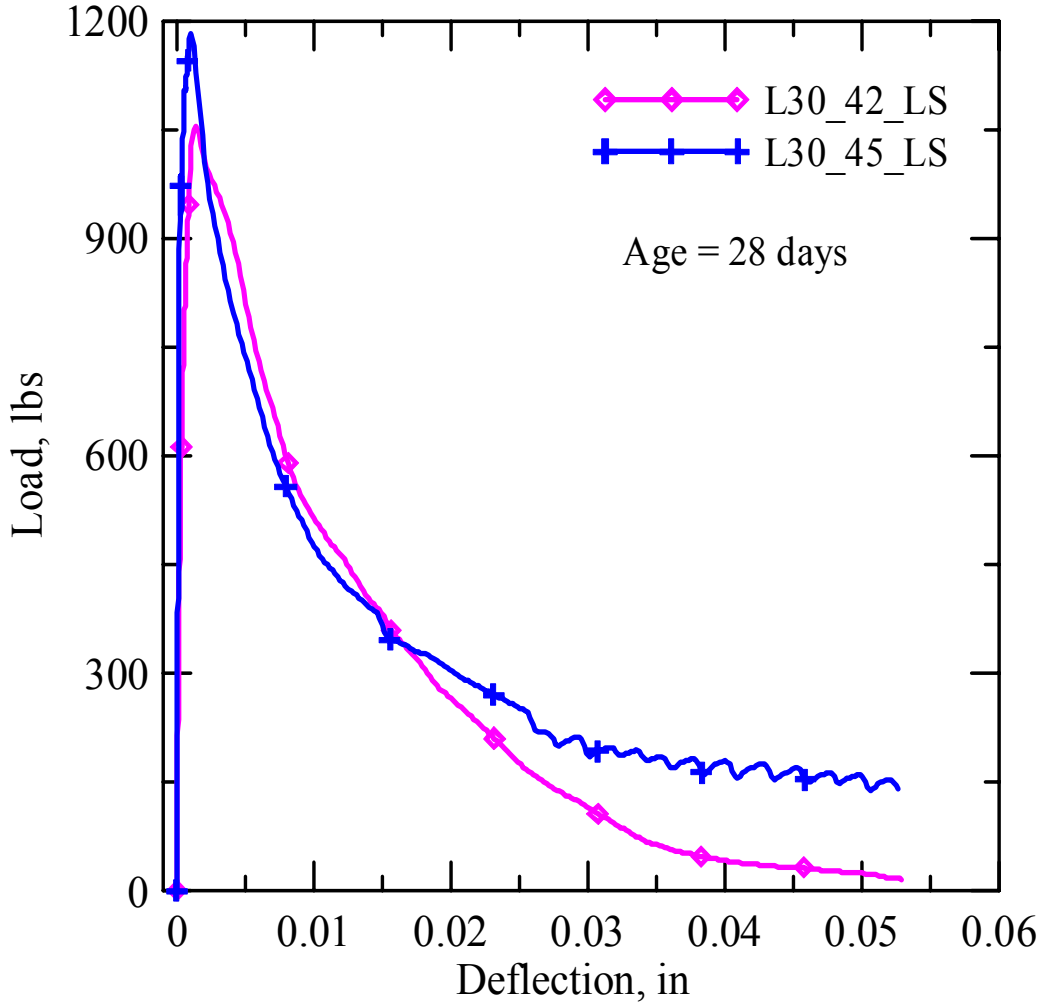

Figure 2.14. Effect of water cement ratio on the flexural Strength

CHAPTER 3

FIELD TRIAL OF THE 30% FLYASH CONCRETE MIXTURES

3.1 Introduction

This chapter discusses the implementation of the experimental mix designs developed in the ASU Lab into the field. The study described in the previous chapter indicates that that mix designs with both high and low cement contents can be developed in the laboratory in order to meet the design guides. From the experimental study of various mixes developed by the ASU Lab, it is seen that the compressive strength of nearly 4000 psi was achieved with the mix design of low cement content (About 490 lbs per cubic yards of concrete with 30% flyash). It was proposed to develop a field trial of type of concrete mixture in order to evaluate its field performance.

Based on the studies conducted, the mix corresponding to L30_42_LS was proposed as the mix design for the field trial as shown in Table 3.8.

3.2 Implementation of the Mix Design in the Field

To implement the above mix design in the field, various pavement test sections were chosen in collaboration with the state agency ADOT. Figures 3.15 and 3.16 show the initial condition of the site before roadwork and before and after sub-base preparation. The project involved using 30 Cubic yards of concrete with 30% flyash to cover a 100 ft test section of the access Frontage to I-10 located at the intersection of Ruthrauff and Sunset Roads in Tucson. The mix design of concrete with 30% flyash according to class P concrete was provided to both ADOT and Mr. Bill Schneider of Tucson ready Mix.

During the course of this project, the following individuals were instrumental in helping with the various phases of the work.

- Mr. Jim Lange, MRT, supplying the flyash
- Mr. Bill Schneider, Tucson ready mix, mix design and delivery
- Mr. Tom Covell, KE&G Construction
- ADOT personnel: Mr. Dave Burbank, Mr. Tony Hanna, Ms. Ligia Liuria, and Several others.

Figures 3.17 through 3.22 represent the various stages of placing and finishing sample collection and curing of the sections. Three different sets of mixture samples were collected during sampling. The field tests were carried out on March 25th, 2002. Various samples were collected at regular interval along the test section of pavement as shown in Figure 3.20 to study the effect of flyash level on the strength, fracture & shrinkage. The only deviation from the standard methods used by the contractor was the specification of the moist curing for the test section. It was required to provide a covering for freshly poured slab to reduce the moisture loss during the seven days moist curing process.

3.3 Samples Collected

To evaluate the reproducibility and consistency of the test results, three different types of mix designs were considered. The first type was prepared with SRP supplied flyash at the 30% level. The second concrete mixture was also containing 30% flyash such that the flyash was locally obtained from Apache power generation plant. The third type was the control mixture, which utilized 20% flyash using the local source used by

Tucson ready mix. The mix designs are represented in Tables 3.9 and 3.10 and abbreviated as follows:

- Tucson Ready mix concrete with SRP 30% flyash in concrete, designated as: TRM_SRP_30FA.
- Tucson Ready mix concrete with 30% flyash in concrete, designated as: TRM_30FA.
- Tucson Ready mix concrete with 20% flyash in concrete, designated as the Control Mixture: TRM_20FA.

For each mix design samples were collected for flexure, compression and shrinkage testing. In addition, test samples for compressive strength were also collected and tested by ADOT engineers. These samples were primarily 6”x12” compression cylinders and were tested at 14, 28 and 56 days respectively. For the samples collected by ASU team, compression test was conducted according to ASTM C469 and flexure test was carried out as Three Point Bending test according to ASTM C78 for all the specimens at the age of 7 and 28 days respectively. Restrained shrinkage test was conducted for the duration of 35 days.

It was noticed that the compaction was an issue especially for some of the initial samples. That is shown by the effect of the air pockets that were observed on the surface of some of samples as shown in Figure 3.23. This may be attributed to the low slump of the mixtures observed during the construction process. Such an effect can be easily handled by adjusting the amount of superplasticizer in order to achieve a desired

rheology of the mix. No attempts were made to change the slump of the mixtures during the construction of pavement.

3.4 Experimental Results

Figure 3.24 presents the stress vs. circumferential strain curve for SRP 30% flyash in concrete at 7 and 28 days. It is observed that there is a 50% increase in strength at 28 days from 7 days with the maximum strength for SRP 30% flyash concrete at 28 days is 3700 psi. The post peak response is also very good which indicate that it has higher ductility and energy absorption capacity. The test result obtained in the Lab for the compression test is shown in Table 3.11.

Figure 3.25 shows the comparison of the results of the uniaxial compression tests carried out in the ASU laboratory and the tests conducted by the ADOT in their lab according to ASTM C 469. Main differences between the two tests include the size of the specimens and also the manner of testing. The size of the specimens tested by ASU was 4”x 8” cylinders in comparison to ADOT tested samples of 6”x12”. Another difference is the method of testing as the ASU tests were conducted as closed loop tests to measure the post peak response of concrete in comparison to simple compression test conducted by the ADOT. In closed loop test, the rate of loading is slower, thus allowing creep to take place, and after the sample is loaded up to a certain load, the test control is transferred to the extensometer (circumferential strain) control in order to avoid the sudden failure of concrete samples. In the simple compression test, the samples are loaded until complete failure of sample is occurred under load. The test results obtained by ADOT are shown in

Table 3.13. From result table, it is seen that concrete cylinders tested by the ADOT reached the compressive strength of above 5000 psi at 28 days.

Figure 3.26 presents the bar graph of compression test result at 7 and 28 days for high and low volume of cement content and various levels of superplasticizer in comparison with the field trials. It is observed that the there is a decrease in compressive strength of concrete from high to low cement content, while the concrete with 30% flyash and low cement content and low superplasticizer meets the strength requirement of Class P concrete with average compressive strength of 4125 psi. It is also observed that the superplasticizer content has no significant effect on the compressive strength except on the rheology of concrete, as there is only 3% - 5% difference in the compressive strength.

The effect of water cement ratio in the range of 0.42 -0.45 is also insignificant as far as the nominal strength values are concerned. The samples with a w/c ratio of 0.45 resulted in reduced strength values, which are as much as 6% lower than the strength of mixtures with w/binder of 0.42.

Figure 3.27 presents the load vs. deflection curve for SRP 30% flyash and Tucson 20% flyash in the concrete at the age of 28 days. The flexure strength at 28 days for SRP 30% flyash is slightly lowers than the Tucson 20% flyash concrete. The post peak response for Tucson 20% flyash concrete is also better than SRP 30% flyash concrete with only 12% increase in toughness, which represents the degree of embrittlement obtained due to the addition of flyash. The toughness as a function of the displacement is shown in Figure 3.28. The test results obtained in the lab of flexure test are shown in Table 3.12.

Figure 3.29 presents a bar graph of the flexure test results at 7 and 28 days for different volume of flyash in concrete and with different superplasticizer content. It is observed that the there is little difference in flexure load of concrete with 30% flyash and the concrete with 35% flyash. This difference is in the range of 5% only. It can be also observed that the superplasticizer has no significant effect on flexure strength, as the flexure strength is almost same for both the low and high superplasticizer content.

Figure 3.30 presents the toughness values at 28 days for different volume of flyash and superplasticizer content. Superplasticizer has no significant effect on toughness, as with the low and high superplasticizer content there is no much difference in toughness value. The concrete with Low superplasticizer and low cement content results in the largest value of toughness of 14 psi.in indicating a comparatively better ductility and energy absorption capacity.

Compared to the test results from previous studies it is concluded that the addition of up to 30 % of flyash does not significantly reduce the performance of concrete mixtures even at the low cement content mixtures studied. The compressive strength test results from ADOT indicate that minimum compressive strength with proposed mix design at the age of 28 days is more than 4000 psi. SRP 30% flyash in concrete gives almost the same strength as that of ADOT 20% flyash in concrete with an advantage of considerable saving of cement in concrete. The proposed mix designs can save up to 40 lbs. of cement per Cu.yd of class P concrete when compared to the mix design of the ADOT.

3.5 Shrinkage Test

To Assess cracking due to restrained shrinkage, a ring type specimen was used to simulate the restrained shrinkage testing. The ring consists of a 2.625 in. thick cylinder of concrete, which is cast around a rigid steel ring with a diameter of 11.4 in. and a height of 5.25 in as shown in Figure 3.31. The specimen were demolded after 24 hrs and then kept for observation in the chamber. Drying was allowed from outer, circumferential surface. Since the height of specimen (5.25in.) was two times to its thickness (2.625in.) it was assumed that uniform shrinkage took place along the height of specimen. The rings were placed in an environmental chamber at a temperature of 104º F (40º C) and inspected for up to 40 days using a continuous recording of the strain in the inner steel by two strain gauges attached to the inner surface of the steel ring. The response from the strain gauge was recorded at every minute. In order to measure the crack width, a special microscope set up was used. The microscope was attached to a frame grabber and pictures of cracks were taken. The surface of the specimen was examined for new cracks and the measurements of the width of already existing cracks at every 24 hours during the first few days after cracking, and then after every 48 hours.

3.5.1 Measurement of Crack Width

A computer-based technique was developed for the measurement of crack width. This automated procedure allowed us to analyze several specimens at a time to measure the average crack width. The procedure for crack width measurement was based on obtaining an image of the crack. The intensity of the pixels determines the existence of a crack. This image was processed, and subjected to segmentation, a process to separate

the crack from the rest of the image by the intensity of the pixels. All the pixels below certain intensity were designated as a crack. The width of the crack was measured by means of intersecting the binary image with a series of parallel lines. The lengths of the resulting segments were measured in terms of pixel length, and after appropriate calibration factors were applied, the results were reported as crack width. Figure 3.32 shows the segments of the binary image obtained after intersection of the parallel lines with the binary image representing the crack from the original photograph.

3.5.2 Shrinkage Result

Figure 3.33 represents the response of strain gages attached to the specimen. These responses are measured as a function of time, and can be used in order to detect the time of cracking in the specimen. Note that initial increase in the strain is because of the high temperature when the specimens are placed in the environmental chamber after curing for 24 hrs. Gradually as the concrete shrinks under given temperature, the strain gauge mounted on the steel ring show compression. With the initiation of crack in the specimen, the concrete expands and finally at the end of the test period as the crack grows throughout specimen, there is no response from the strain gauges in the rest of the period. From the plot it is seen that specimens with 20% Flyash had first visible crack at the age of 10 days, while for specimens with 30% flyash had first crack at the age of 8 days.

Figure 3.34 presents the crack mosaic in various specimens during restrained shrinkage test and figure 3.35 presents the graph of Average crack widths vs. Age obtained from the crack width measurement by Math lab program. From this figure it is

clear that the crack width of SRP 30% flyash specimen is less compared to other specimens. The specimen containing SRP 30% flyash has first visible crack at the end of nearly 8 days and it is measured as 0.0085 in. wide. It was observed that once crack became visible, it propagated quickly through the whole thickness of the ring. In addition, only a single crack was developed throughout the observation period. This crack dominates the formation of any other crack in the specimen. The results of crack width measured for various samples are shown in Table 3.14.

Table 3.8

Proposed Mix Design for the Field Trials (4000 psi Class-P W/AIR)

Mix ID #	% FA	% Air	Slump in	Cement Content lbs/Cu.yd	W/B	Dry weight of materials, lbs				
						Cement	Flyash	Water	Sand	CA
L30_42_LS	30	3	2”	493	0.42	493.4	148.1	269.6	1273.8	1677.7

Table 3.9

Summary of the Mix Formulations used in the Field Trials

Mix ID	Cement Content	FA Source	% FA Content	W/C
TRM_20FA	Low	Apache power generation plant	20	0.42
TRM_SRP_30FA	Low	SRP	30	0.42
TRM_30FA	Low	Apache power generation plant	30	0.42

1) TRM refers to Tucson ready Mix Concrete

2) SRP refers to Salt River Project

Table 3.10

Mix Design of Concrete used in the Field Trials

MIX ID	% FA	TA/ (C+FA)	Cement Content lbs/yd^3	Flyash Content lbs/yd^3	W/B	Cement lbs	Flyash, lbs	Water, lbs	Sand, lbs	CA, lbs
TRM_20FA	20	4.56	534	113	0.43	533.5	112.4	282.8	1184.7	1764.8
TRM_SRP_30FA	30	4.6	492	147	0.42	491.6	147.7	273.4	1268.5	1669.1
TRM_30FA	30	4.6	492	147	0.42	491.6	147.7	273.4	1268.5	1669.1

Table 3.11

Compression Test Results of the (4" x 8") Cylinders

MIX ID #	Age Days	% FA	Strength psi	Strain at Peak Load in/in 10E-04		Modulus of Elasticity psi 10E+06	Poisson's Ratio
				Axial	Lateral	Axial	
TRM_SRP_30FA	7	30	2553	1.68	3.87	4.63	0.22
TRM_SRP_30FA	28	30	3701	1.41	1.13	8.47	0.25

Table 3.12

Measured Material Properties from Three- Point Bending Test

Mix ID #	% FA	Age days	At the Peak Load				Toughness psi.in
			Load lbs	Effective Stress psi	CMOD in 1.0E-03	Deflection in 1.0E-03	
TRM_SRP_30FA	30	7	995.91	325.2	1.319	2.168	7.2
TRM_ 20FA	20	7	1030.2	336.4	1.1187	1.2443	8.7
TRM_SRP_30FA	30	28	1023.6	334.24	1.1637	1.1871	8.5
TRM_20FA	20	28	1047.1	341.91	1.1167	2.095	10

Table 3.13

Result obtained from ADOT (6" x 12")

Mix ID	Slump	Age	Peak Load	Max. Strength	Avg. Strength
		days	lbs	psi	psi
TRM_SRP_30FA	1/2"	14	143010	5040	5010
			140950	4970	
		28	152090	5360	5220
			146850	5180	
		56	156260	5510	5330
			146210	5150	
TRM_ 30FA	1/2"	14	121080	4270	4320
			123630	4360	
		28	147140	5190	5030
			138340	4880	
		56	137550	4850	4730
			130730	4610	
TRM_ 20FA	1/2"	14	136190	4800	4610
			125510	4420	
		28	148800	5240	5320
			153290	5400	
		56	156660	5520	5250
			141150	4980	

Table 3.14

Average Crack Width Measurements for the Shrinkage Test

Date	Age days	Concrete Mix	Average Crack Width mm	Standard Deviation
4/9/2002	10	TRM_20FA	0.701	0.084
		TRM_SRP_30FA	0.216	0.083
		TRM_30FA	0.305	0.051
4/24/2002	25	TRM_20	0.961	0.071
		TRM_SRP_30FA	0.311	0.023
		TRM__30FA	0.463	0.086
5/6/2002	35	TRM_20FA	0.983	0.081
		TRM_SRP_30FA	0.342	0.032
		TRM_30FA	0.503	0.062

Figure 3.15. The access road prior to roadwork alignment

Figure 3.16. The access road during sub base preparation

Figure 3.17. The completed sub-base prior to placement of concrete

Figure 3.18. The dowel bars for the connection of the new slab with the existing slab

Figure 3.19. Concrete pouring in test section of pavement

Figure 3.20. Collection of test samples from pavement sections

Figure3.21. Test section of pavement during poring of the high flyash mixtures

Figure 3.22. Covering of the freshly poured slab to reduce the moisture loss during seven days moist curing process

Figure 3.23. Lack of consolidation observed in samples collected at the field

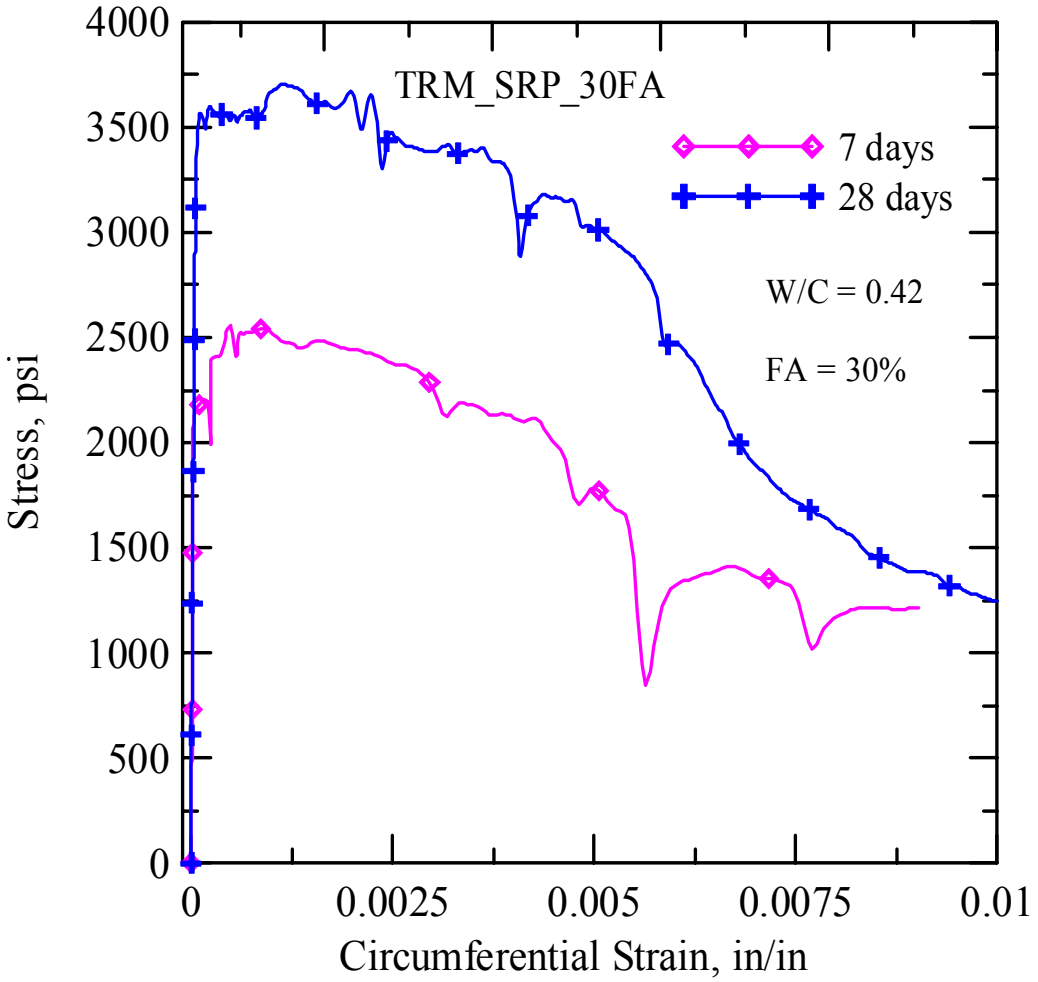

Figure 3.24. Stress vs. Circumferential Strain for SRP 30% FA in concrete

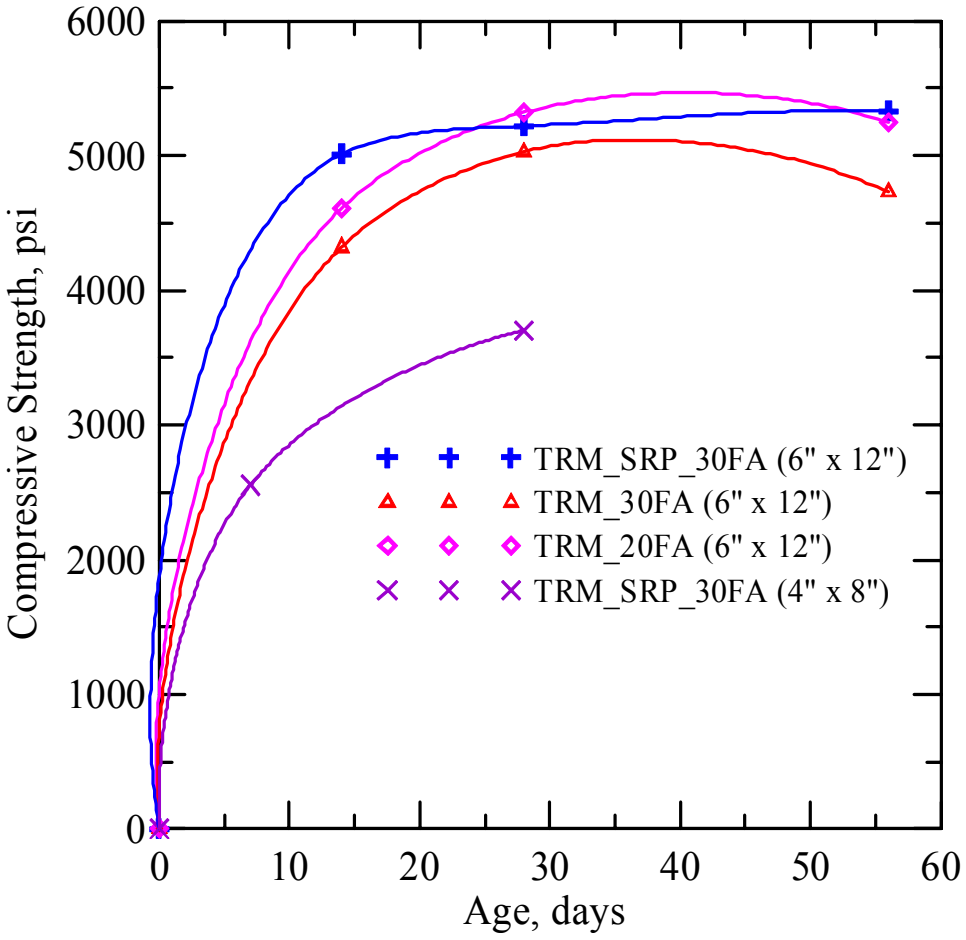

Figure 3.25. Comparison of compressive test results with age

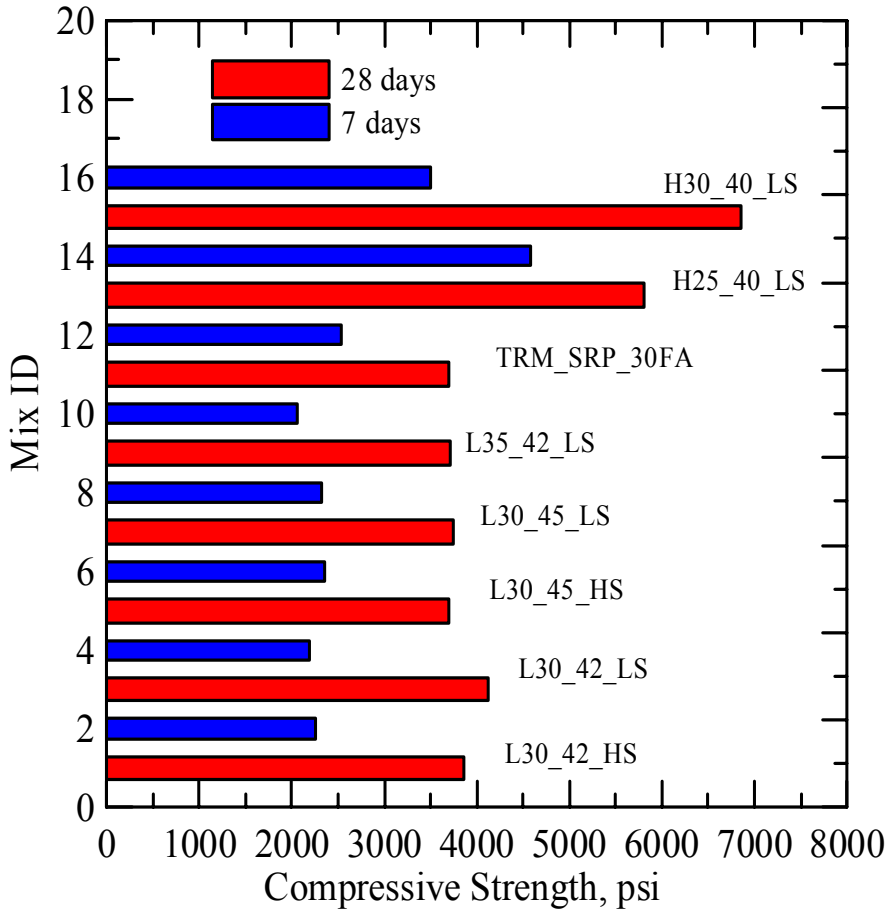

Figure 3.26. Comparison of compression test result at 7 and 28 days with respect to volume of cement content

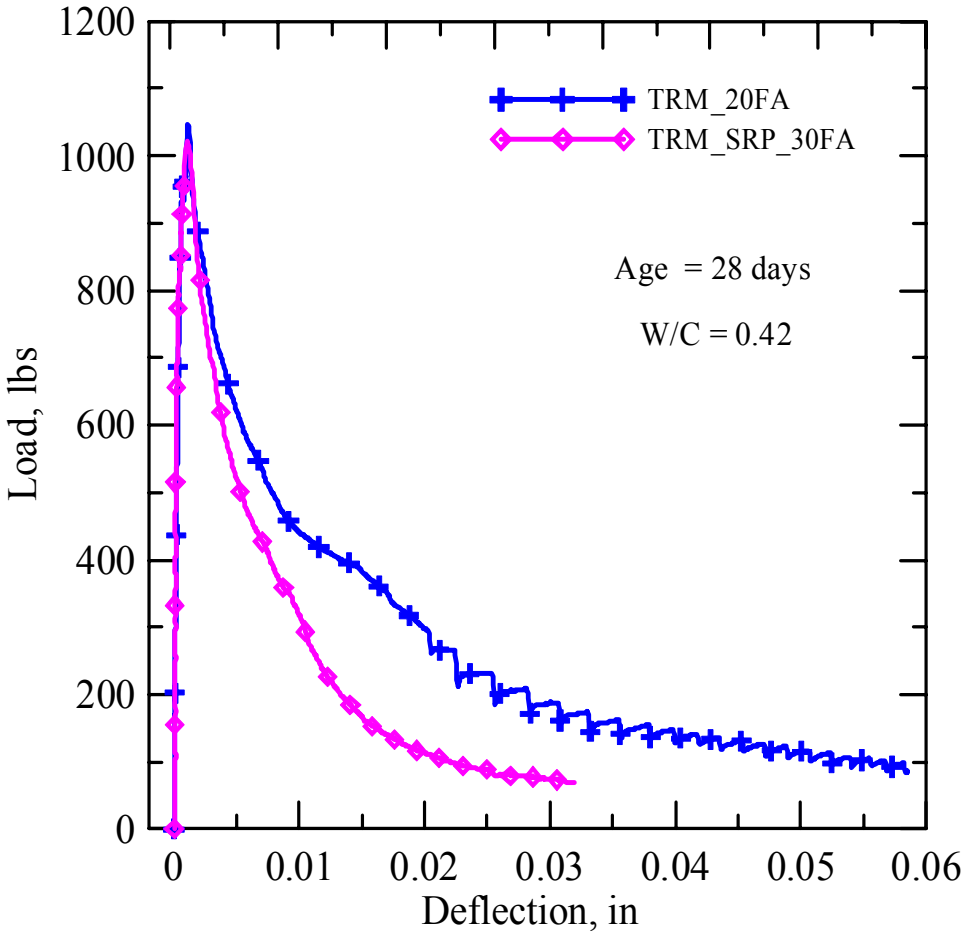

Figure 3.27. Load vs. Deflection for SRP 30% and Tucson 20% FA in concrete

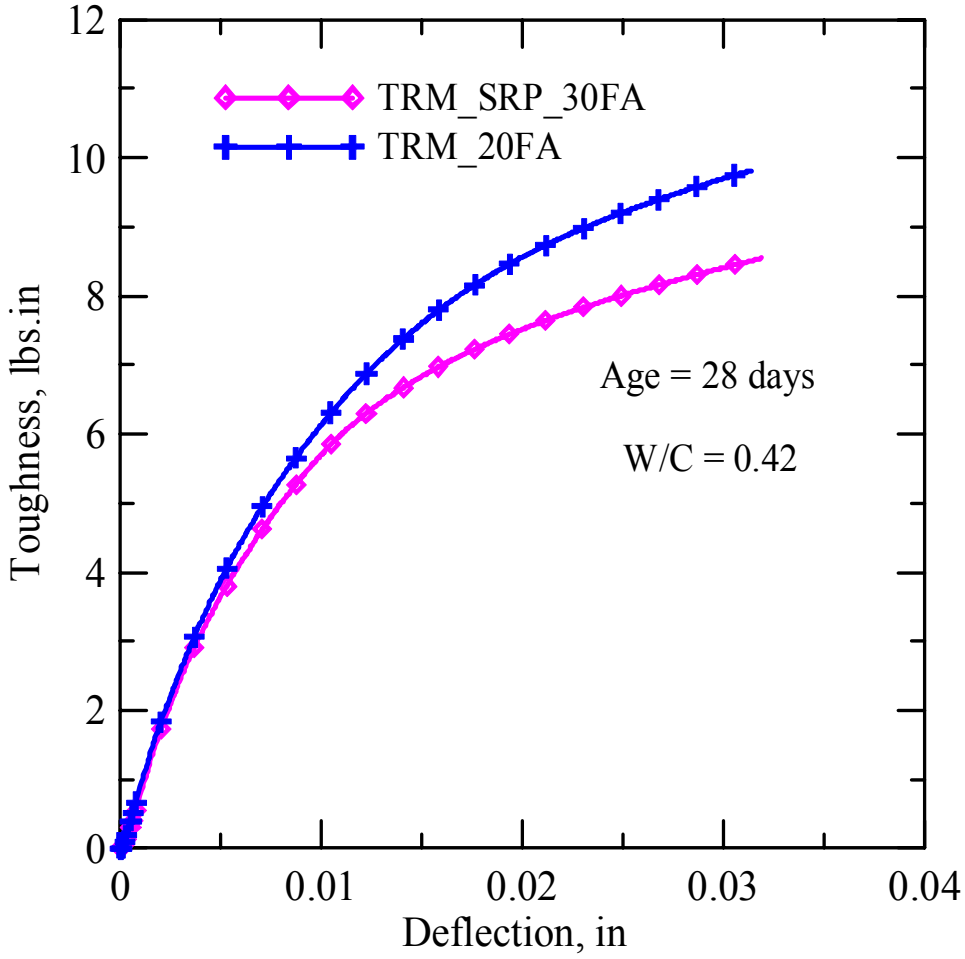

Figure 3.28. Toughness vs. Deflection for SRP 30% FA and ADOT 20% FA in concrete

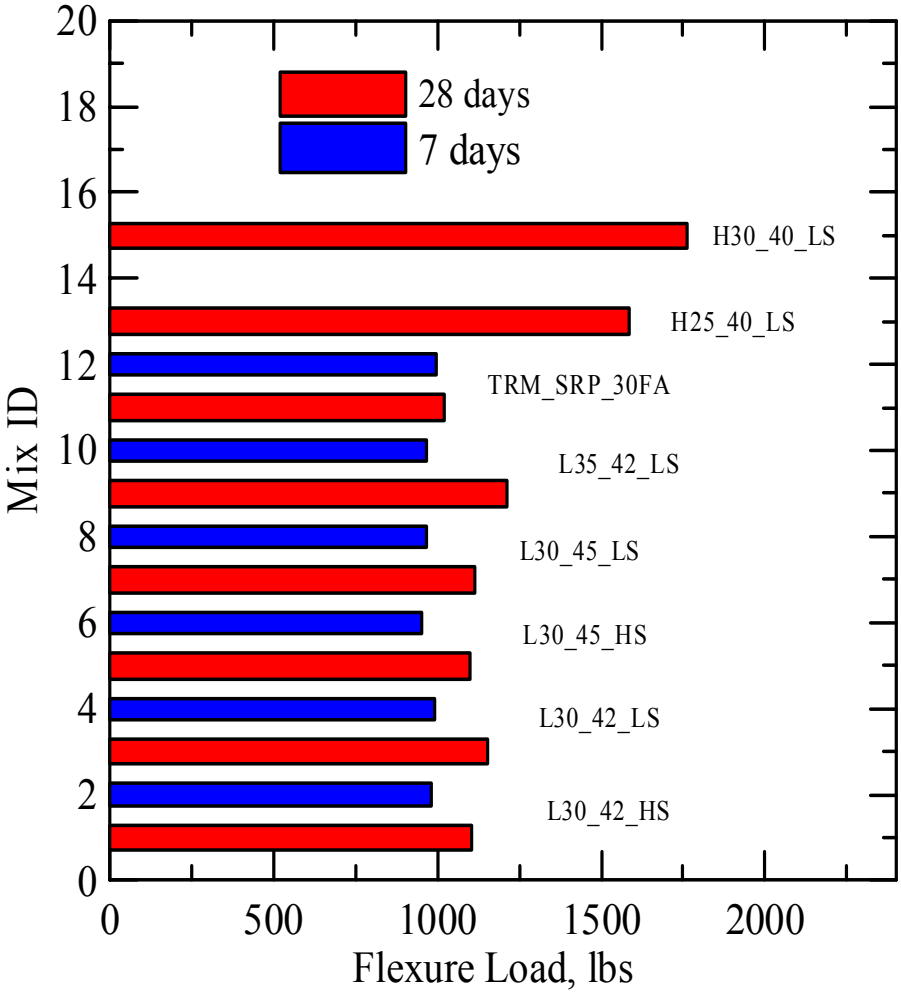

Figure 3.29. Comparison of flexure test result at 7 and 28 days with respect to volume of flyash and superplasticizer content

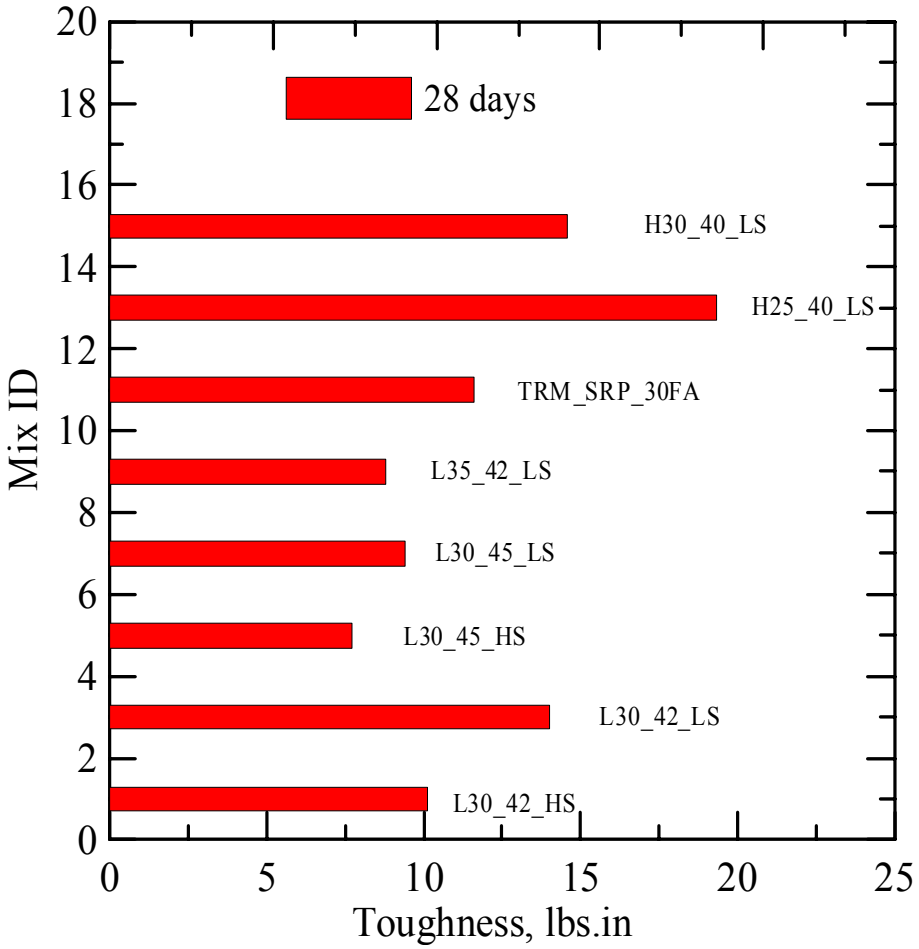

Figure 3.30. Comparison of toughness at 28 days with respect to volume of flyash and superplasticizer content

Figure 3.31. Restrained shrinkage specimens during the test

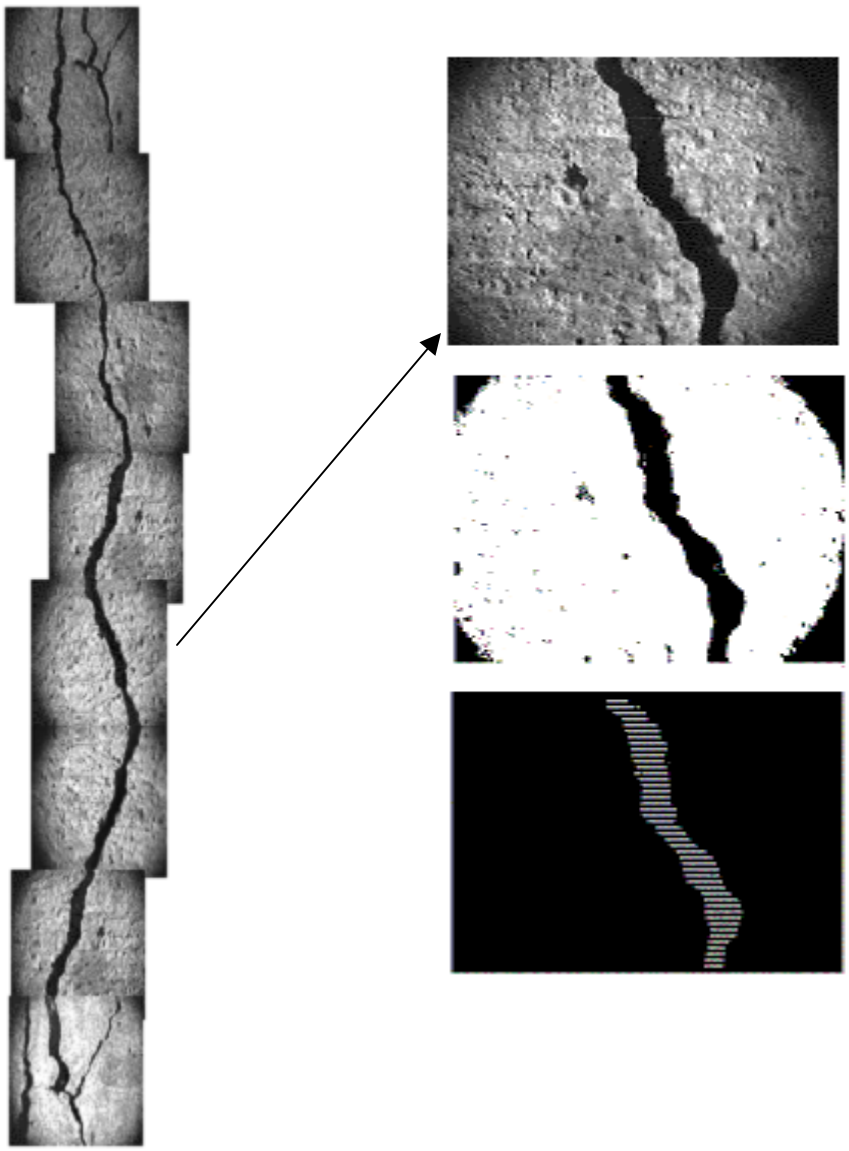

Figure 3.32. Showing various stages of measurement of crack width of shrinkage specimen (TRM_30FA) by Math lab program.

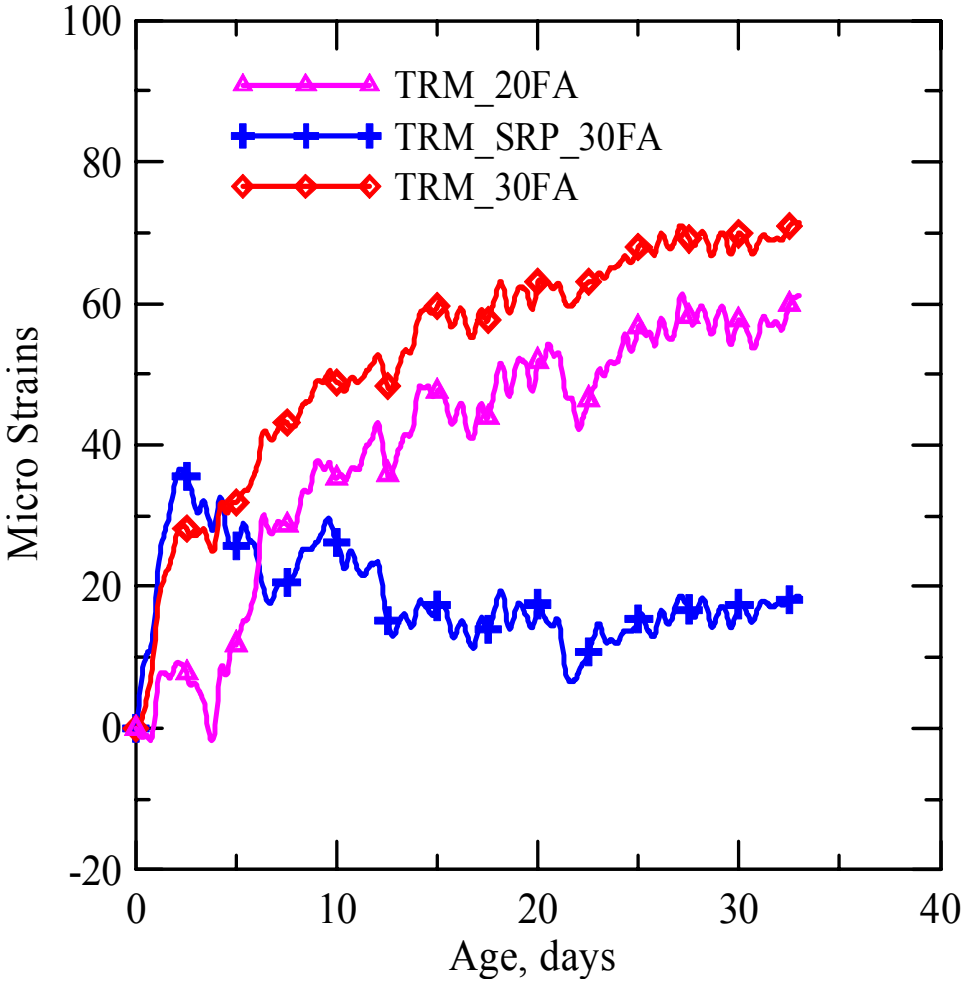

Figure 3.33. Restrained shrinkage strains vs. duration of shrinkage

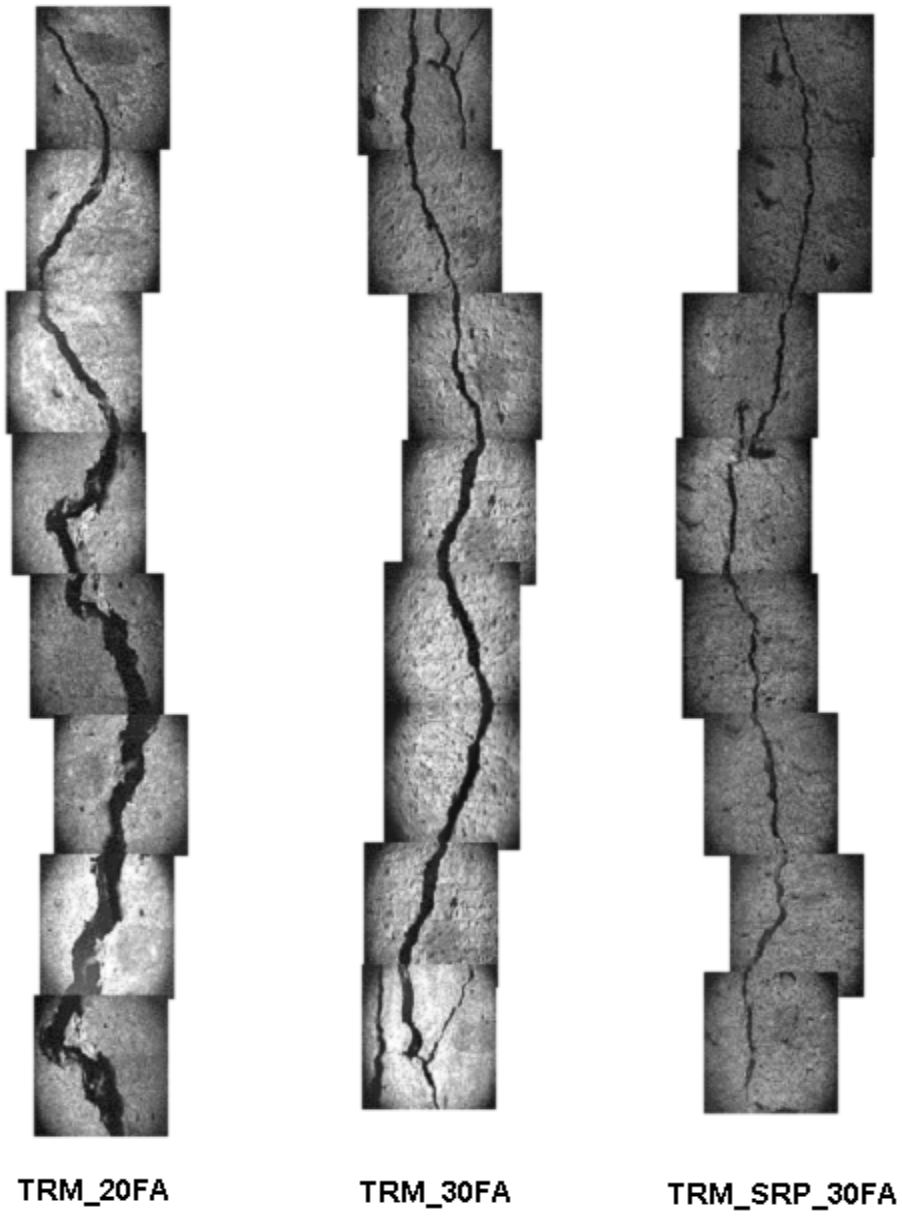

Figure 3.34. Crack mosaic in shrinkage specimens

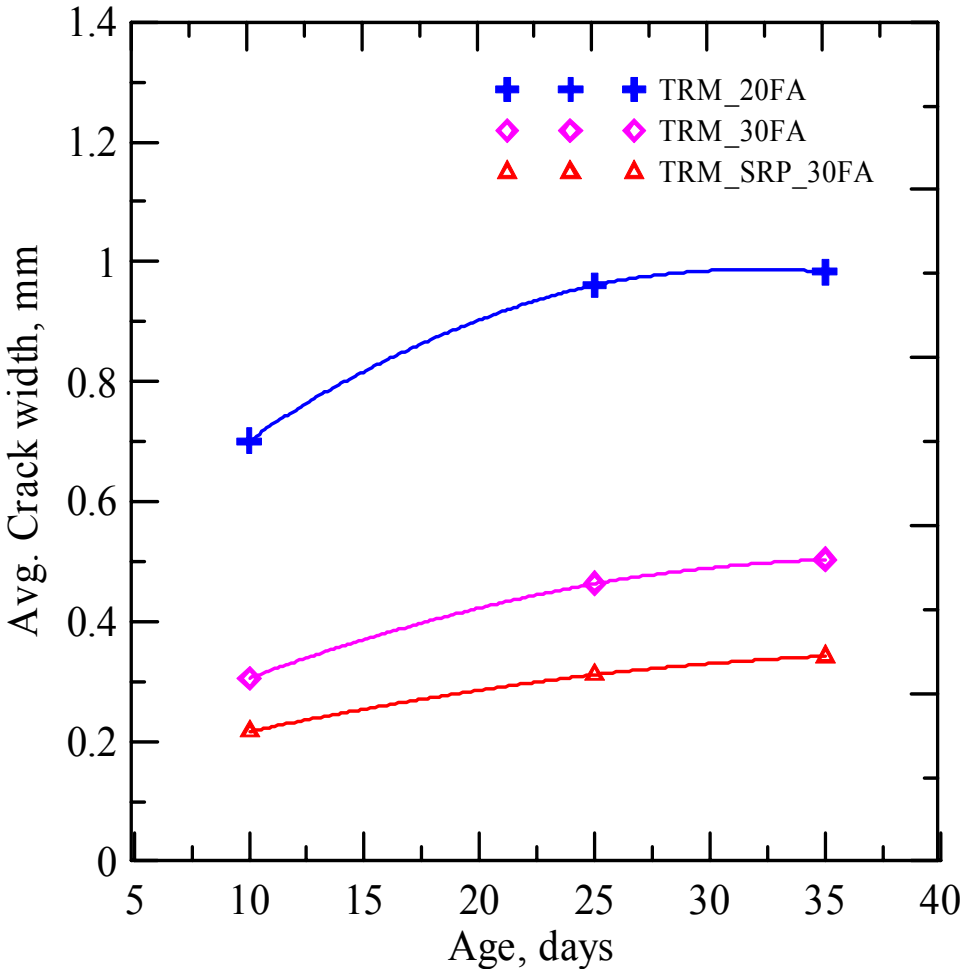

Figure 3.35. Average crack widths vs. Age for shrinkage specimen

CHAPTER 4

MECHANICAL BEHAVIOR OF ALKALI-RESISTANT GLASS FIBER CONCRETE

4.1 Introduction

This chapter discusses the mechanical properties of a concrete reinforced with AR Glass fibers. Compression and flexural properties of FRC (Fiber Reinforced Concrete) were studied. An experimental study was conducted to evaluate the effects of glass fibers of various types, lengths and contents. A hybrid fiber reinforcement system with various lengths of fiber was also examined.

4.2 Experimental Work

4.2.1 Fiber Types

Two types of AR Glass fibers, HP and HD were used. These fibers were obtained from VETROTEX, Cem-FIL SAINT-GOBIN. High dispersion (HD) AR Glass fibers are used in chopped strand form, which disperse thoroughly throughout the mixtures. These fibers are formulated for mixing with concrete, mortar and other cement based mixes where a uniform dispersion is of great importance. These fibers are more effective in controlling and prevention of early shrinkage plastic cracking. They produce a more homogeneous concrete matrix, with rapidly disperse in the mix, and produce a smooth finish. High performance (HP) AR-glass fibers maintain the bundle characteristics throughout the mixing and casting with increase in concrete's flexural strength, tenacity, ductility, toughness, impact and abrasion resistance, and are highly resistant to degradation during mixing. These fibers enhance the properties of hardened concrete

under loads. Typical mechanical properties of fibers used for the present study are given in Table 4.15.

4.2.2 Specimen Preparation

A Concrete mix design was developed for the production of HPC. The water-binder ratio was 0.4 with characteristic strength of 6000 psi and slump of 2 to 2.5 in. used. Class F flyash equivalent to 10% cement replacement was also used. The mix design of concrete used is shown in Table 4.16. In order to achieve a desired slump and cohesive concrete mix, the following mixing procedure was adopted. The dry coarse aggregate and sand were introduced in the mixer and blended for 90 seconds with superplasticizer and half of the mixing water. Then, cement, flyash, fiber and remaining water added to the mixer and blended for 3 additional minutes to thoroughly mix all the ingredients. All the specimens were filled in two layers with proper compaction in between the layers. A vibration table was used to help with the consolidation of the fresh mixture in the molds.

The dosage of high dispersion (HD) AR Glass fibers was limited to 20 Kg/m^3. The content of high performance (HP) Glass fibers was 10 Kg/m^3 and 20 Kg/m^3.

Several different lengths of fibers, 6, 12, and 24 mm were used for HP fibers, while for HD fibers only 12 mm fiber length was used. Specimens were prepared for each length of fiber in addition; a hybrid fiber reinforcement system containing various lengths of fibers, 6, 12 and 24 mm of HP Glass fibers was developed. Several hybrid systems were prepared: 1) HP6,12 2) HP6,24 3) HP12,24 4) HP6,12,24. The fibers in the hybrid

systems were equally distributed (by volume) in the mix. In all hybrid systems the content of fiber was 10 Kg/m^3.

Specimens were tested for both compression and flexure (Three point bending) tests. The experimental procedure for closed-loop compression test and flexure test was described in detail in 2.4 (Test Procedure and Results in CH 2). For hybrid fiber reinforcement system only flexure test was used. The size of specimens prepared for compression and flexural tests were:

1) Flexure Tests - Beams were prepared with dimension of 14 x 4 x 4 in.

2) Compression Test - Cylinders were prepared with dimension of 3 x 6 in.

The Specimens were cured for various ages at 3,7 and 28 days up to testing for compression test and only 28 days for flexure test.

A summery of all the specimens prepared including test method and curing is shown in Table 4.17. In this table Mix.ID presents the type of fiber (HP or HD), fiber length (6,12 or 24 mm) and fiber content (10 or 20 Kg/m^3). For example HP12_10 presents the specimen produced from HP fibers with a length of 12 mm and fiber content of 10 Kg/m^3 and HP1224_10 presents specimens produced from HP fibers with lengths of 12 mm and 24 mm (50%-50%) and fiber content of 10 Kg/m^3.

4.3 Experimental Results

4.3.1 Compression Test Results

Analysis of the compression test results was conducted to evaluate the effect of fibers length, fibers volume and aging on compressive strength of the fiber reinforced concrete mixes. A summery of the experimental results is shown in Table 4.18.

Figure 4.36 represents the Stress vs. Circumferential Strain for specimens containing 10 Kg/m^3 and 20 Kg/m^3 of HP12mm AR glass fiber for various ages at 3, 7 and 28 days. Response of this specimen indicates several distinct regions. The first region is the initial linear ascending stress strain response. The second region is due to initiation of microcracks that results in a reduction in the stiffness and thus the non-linear behavior of the specimen. This zone terminates at the ultimate strength. In post peak region, it is observed that there is significant ductility in the circumferential strain pointing out the effect of dilatation. The effect of duration of curing is clearly shown in this figure by a significant increase in the strength and toughness of the composite with aging, in both fiber content systems. This is due to the ability of the fibers to bridge the microcracks in the pre-peak region of the response.

Figure 4.37 shows the effect of fiber volume fraction on the strength and ductility of the FRC with HP12 mm fibers. It is noted that with the increase in volume fraction of fibers, the strength is increased, but there is not much increase in the toughness for concrete with higher fibers content. It is observed that the contribution of the fibers in the post peak region of the high volume fraction is not as much as the case with the lower volume fraction. This is due to the higher strength, a higher magnitude of energy is released, and resulting in strengthening but with added brittleness since the fibers are unable to absorb the energy released as the specimen enters the post peak response for higher volume fraction of fibers.

Figure 4.38 shows the stress vs. circumferential strain for concrete containing HP12-24 (50% -50%) fibers for various ages at 3,7 and 28 days. It is observed that the

increase in strength from 3 to 7 days is significant than from 7 to 28 days. There is an increase of 35% in strength from 3 to 7 days. The post peak response at 28 days is better than at 3 days. The hybrid system of concrete containing of HP12-24 (50% -50%) fibers is more effective in early age strength than strength at 28 days. But at the same time a better toughening of the system is observed, this is mainly after 28 days of aging.

4.3.2 Flexure Test Results

Analysis of the flexural test results was conducted to evaluate the effect of fibers length, fibers volume and type of fibers on flexural load carrying capacity and fracture properties of the fiber reinforced concrete. The present study mainly focuses on the effects of high volume fractions of fibers and fiber length on fracture properties of fiber reinforced concrete. A summery of the results of flexural tests is shown in Table 4.19

Figure 4.39 shows the effect of fibers volume fraction of HP glass fibers on flexural response of FRC. It is noticed that there is a significant increase in the flexural response of the concrete with the increase in the amount of fibers. The flexural strength of the FRC with 20 Kg/m^3 of fibers increases by nearly 100% with respect to control sample and 35% with respect to 10% volume fractions of fibers. The post peak response is also better for the beam with 20 Kg/m^3 of fibers than for the control and 10 Kg/m^3 of fibers volume fraction. This shows a better ductility and energy absorption capacity of the FRC with increase in volume fraction of fibers.

Figure 4.40 shows the flexural response of the FRC with various lengths of fibers at the volume fraction of 10 Kg/m^3 fibers. It is shown that the flexural response of the FRC increases significantly with the addition of fibers. Figure 4.41 shows the effects of

length of fiber on flexural load and toughness. It is shown that there is not much effect on the flexural load capacity when increasing the length of fibers. However there is a significant decrease in the toughness when increasing the length of fibers. The decrease in toughness is around 40% from HP6 to HP24 mm. This behavior might be due to difference in the mode of failure of fibers. The shorter fiber failed mainly by fiber pullout whereas the longer fiber failed mainly by fiber fracture. Fiber fracture produces more energy than fiber pullout.

Figure 4.42 shows the flexural response of FRC as a function of age for HP12 mm with 20 Kg/m^3 of fibers. From the figure it is evident that the flexural response increases with the age having better strength after 28 days. However, there is a very little gain in strength from 7 to 28 days. The increase is mainly in strength whereas the increase in the toughness value is not significant. Moreover, the post peak behavior is slightly better for the early age specimens. This means that the energy absorption capacity of the samples does not increase in proportion with increase in the strength. One possible explanation for this behavior is that during early ages the mechanism of failure is determined by fiber pullout as opposed to fiber fracture at later stages. Fiber pullout dissipates more energy than fiber fracture.

Figure 4.43 shows a comparison between HP12, HD12 and control samples at w/c ratio of 0.4. It is noticed that the performance of the concrete with HP12 is much better than the other two mixes. The increase is in both flexural load and toughness when comparing the concrete with the control and HD12 fibers. The increase in toughness of the HP12 fiber concrete compared with the HD12 fiber concrete specimen is more

significant than the increase in strength. This is due to the bundle effect and fiber pull out, resulting in energy absorption mechanisms. In comparison the HD fibers serve to provide strengthening function due to the good dispersion and bond characteristics.

Figure 4.44 shows the flexure response of concrete with hybrid system of HP12-24 (50%-50%) with different volume fractions compared with the control specimen. From the figure it is evident that the concrete with 10 Kg/m^3 fibers gives the optimum result in strength as compared to the control and the concrete with 20 Kg/m^3 samples, while the post peak response of concrete with the 20 Kg/m^3 is much better than the control and 10 Kg/m^3 of fibers system. So, higher volume fraction is more effective in gaining toughness than strength for this fiber system.

Figure 4.45 shows a bar graph comparing the flexural load carrying capacity and figure 4.46 shows a bar graph comparing the toughness of different mixes as a function of mean fiber length with same volume fraction of 10 Kg/m^3 fibers. It is evident that the FRC with HP12-24 (50%-50%) gives the maximum load capacity as compared to other fiber systems as shown in Figure 4.45 while, the FRC with HP6-24 (50%-50%) gives the best toughness value compared with the other fiber systems as shown in Figure 4.46. Test results indicates that the increase in mean fiber length increasing the flexural load capacity. However, further increase in the average fiber length, resulted in a reduction of the toughness.

Table 4.15

Mechanical Properties of Fibers used for the Present Study

Fiber	Length of Fibers mm	Diameter, Micron	Tensile Strength MPa	Elastic Modulus GPa	Ultimate Elongation, %	Density G/cm^3
Glass (AR)	6,12,24	12	150-380	70	1.5-3.5	2.5

Table 4.16

Mix design of the concrete used

Dry weight per m^3	Kg
Cementitious materials (Cement + flyash)	876
20-10 mm Aggregates	460
10-5 mm Aggregates	300
Fine Aggregates	578
Water/Cement Ratio	0.4

Table 4.17

Summery of Mix designs of the Fiber Reinforced Concrete Prepared

MIX ID	Fiber Length	V_f	Compression Test			Flexure Test
	mm	Kg/m^3	Age of Curing			Age of Curing
			3 days	7 days	28 days	28 days
Control	NA	NA	-	-	-	3
HP6_10	6	10	-	-	-	3
HP12_10	12	10	2*	2	2	3
HP24_10	24	10	-	-	-	3
HP612_10	6,12	10	-	-	-	3
HP624_10	6,24	10	-	-	-	3
HP1224_10	12,24	10	2	2	2	3
HP61224_10	6,12,24	10	-	-	-	3
HP1224_20	12,24	20	-	-	-	3
HP12_20	12	20	2	2	2	3
HD12_20	12	20	-	-	-	3

1) * - In the column of age of curing presents the number of samples tested

Table 4.18

Compression Properties of the different Cylinder Specimens

MIX. ID	Fiber	Age days	Fiber Length mm	Vf Kg/m^3	Compressive Strength psi	Peak Axial Strain in/in	Peak Circumferential Strain in/in	Axial Modulus of Elasticity psi	Poisson's Ratio
HP12_10	AR Glass	3	12	10	2118	1.24E-04	2.28E-04	2.5E+06	0.18
HP12_10	AR Glass	7	12	10	3840	7.39E-04	4.66E-04	5.5E+06	0.22
HP12_10	AR Glass	28	12	10	4996	2.1E-03	5.29E-03	6.3E+06	0.28
HP12_20	AR Glass	3	12	20	2462	2.87E-04	1.03E-04	6.7E+06	0.16
HP12_20	AR Glass	7	12	20	3729	1.03E-04	4.82E-04	4.5E+06	0.23
HP12_20	AR Glass	28	12	20	5768	6.21E-04	2.54E-04	9.9E+06	0.18
HP1224_10	AR Glass	3	12,24	10	3381	4.57E-04	3.79E-04	6.6E+06	0.18
HP1224_10	AR Glass	7	12,24	10	4615	6.15E-04	1.11E-04	5.1E+06	0.27
HP1224_10	AR Glass	28	12,24	10	4643	1.20E-03	9.67E-04	4.7E+06	0.22

Table 4.19

Flexural Properties of the FRC Beams

MIX ID	Ages days	Fiber Length mm	V_f Kg/m^3	Avg. Load lbs	Strength psi	Avg. CMOD in 1.0E-03	Avg. Deflection in 1.0E-03	Avg. Toughness psi.in
Control	28	NA	NA	1272 (66.50)*	311.7	1.204	1.486	9.65
HP6_10	28	6	10	1795 (60.47)	439.7	1.223	1.481	15.88
HP12_10	28	12	10	1785 (100)	437.14	1.236	1.584	16.53
HP24_10	28	24	10	1894 (76.98)	463.94	0.858	0.975	10.10 (166)
HP12_20	28	12	20	2442 (76.33)	598	1.296	3.247	39.18
HD12_20	28	12	20	2330 (125.60)	571	1.21	1.418	14
HP612_10	28	6,12	10	1737 (79.20)	425.6	1.235	1.70	14.42
HP624_10	28	6,24	10	2076 (190)	508.4	0.703	1.290	16.67
HP1224_10	28	12,24	10	2110 (47)	516.7	1.382	0.718	13.22
HP61224_10	28	6,12,24	10	1934 (73)	473.6	0.998	1.505	15.23
HP1224_20	28	12,24	20	1666 (126.12)	408.15	2.52	2.36	23

1) * Numbers in parenthesis reflect the standard deviation of three replicate samples

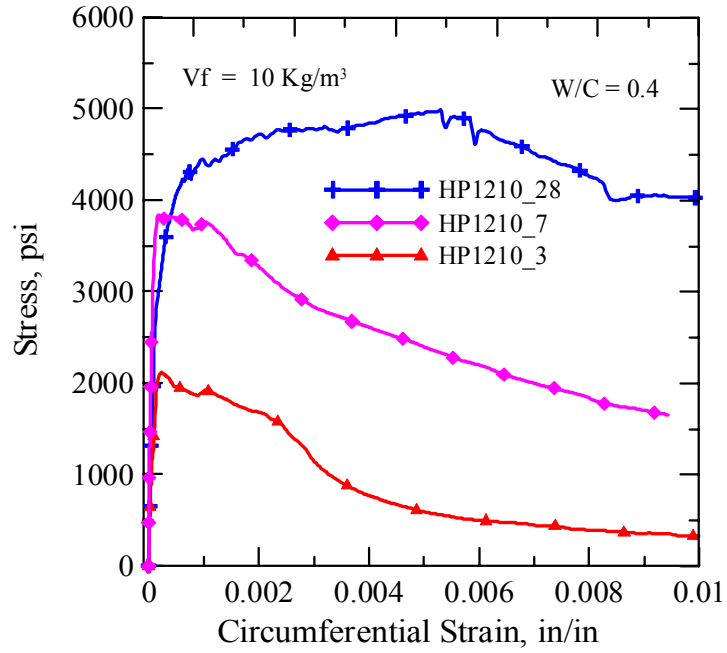

a) Effect of age on compressive stress strain of FRC with 10 kg/m^3 of fibers

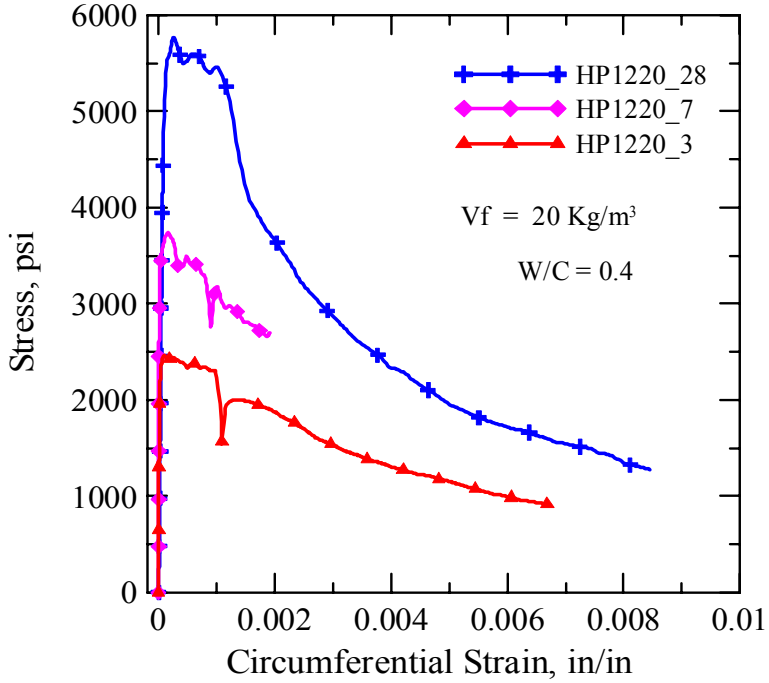

b) Effect of age on compressive stress strain of FRC with 20 kg/m^3 of fibers

Figure 4.36. Effect of age on the compressive stress strain response of FRC

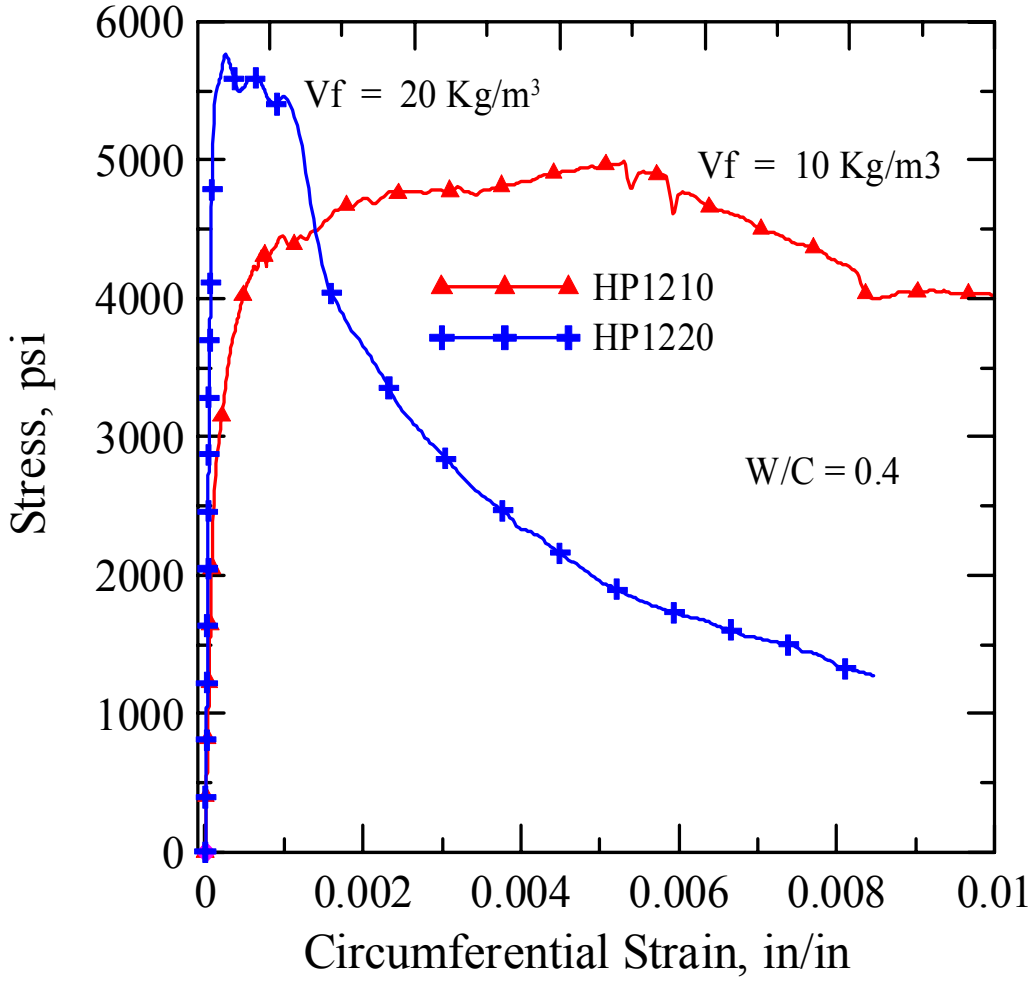

Figure 4.37. Effect of fiber volume fraction on strength and ductility of FRC with HP12 mm fibers

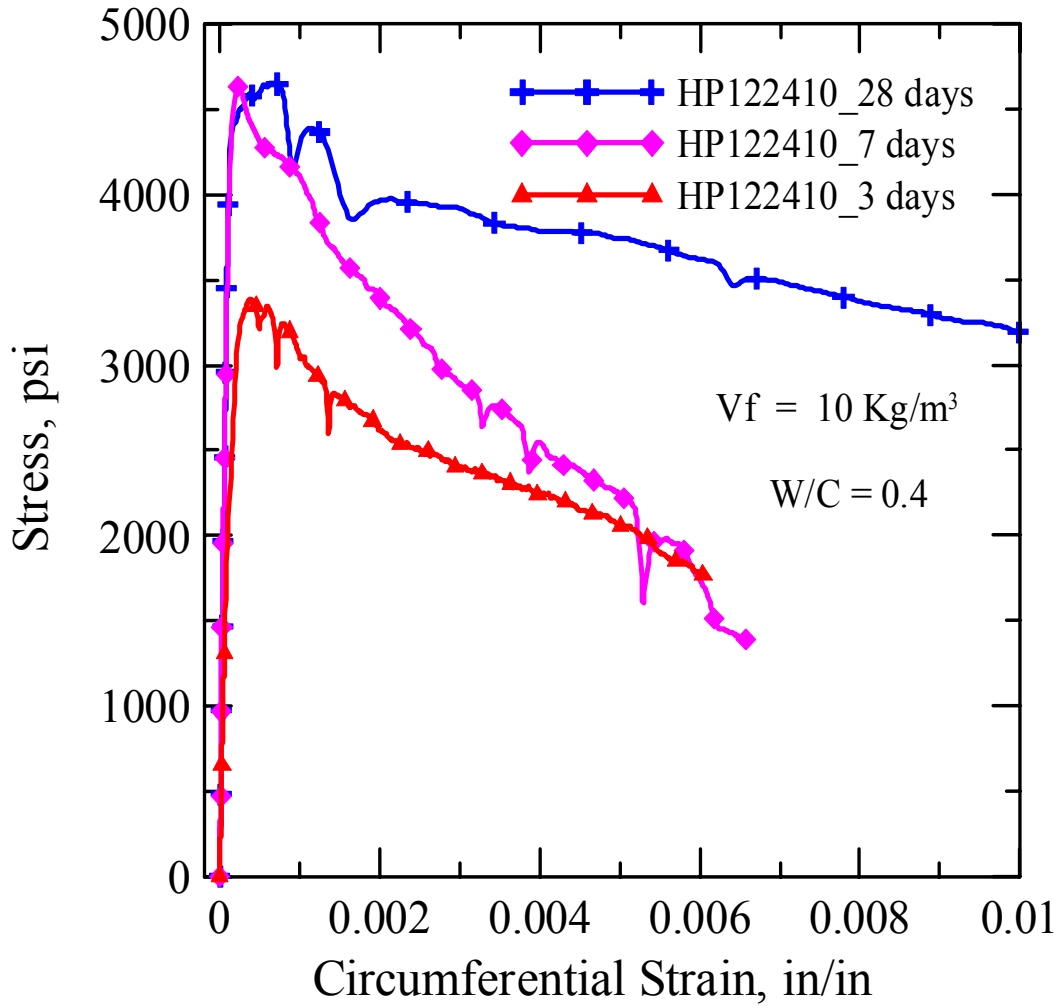

Figure 4.38. Stress vs. Circumferential Strain curve for FRC with HP12-24 (50%-50%) at 3, 7 and 28 days

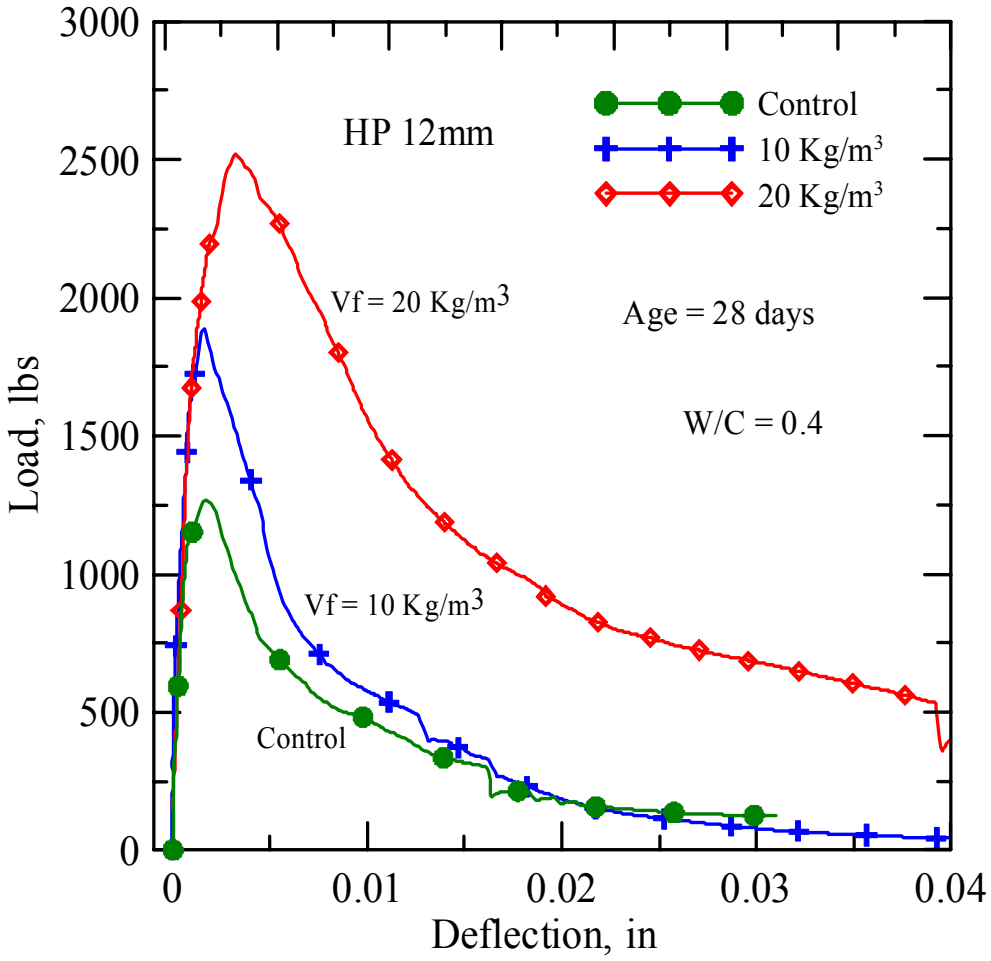

Figure 4.39. Load vs. Deflection of FRC with different volume fraction of HP12 mm fibers

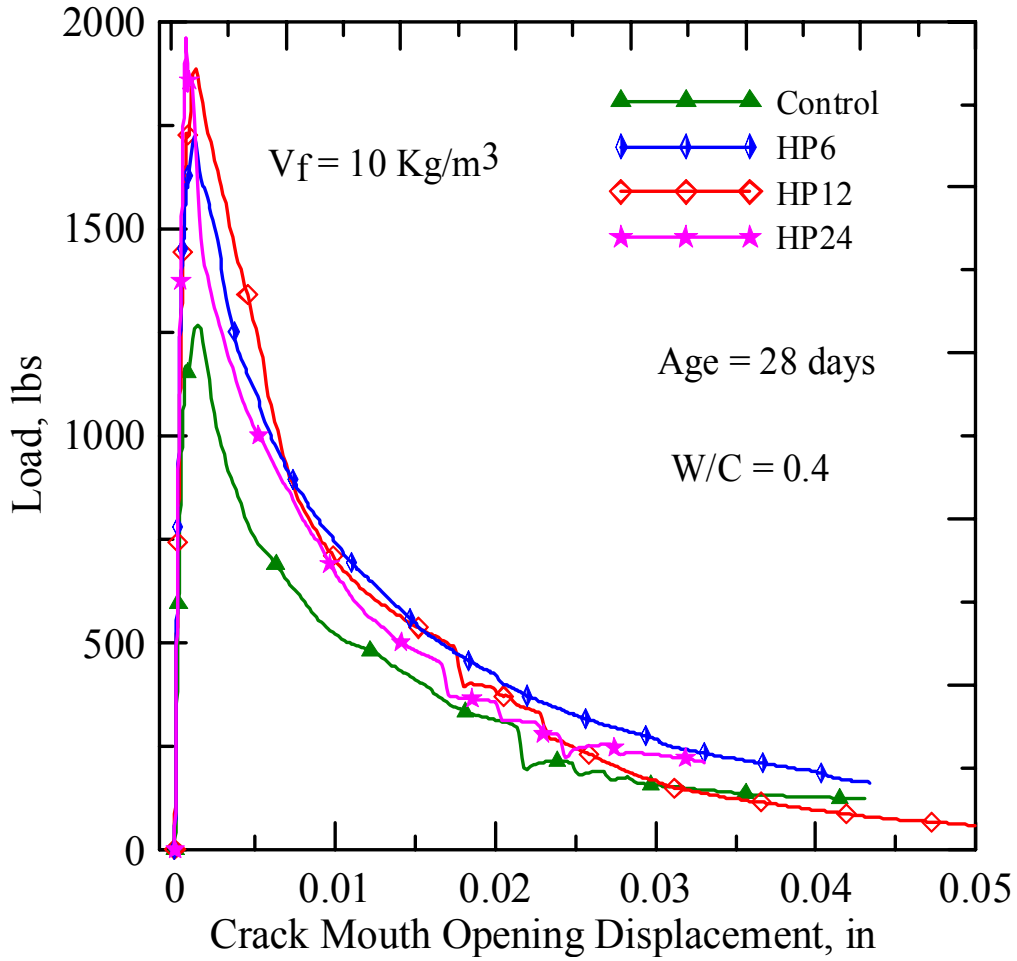

Figure 4.40. Load vs. Deflection of FRC with different length of HP fibers

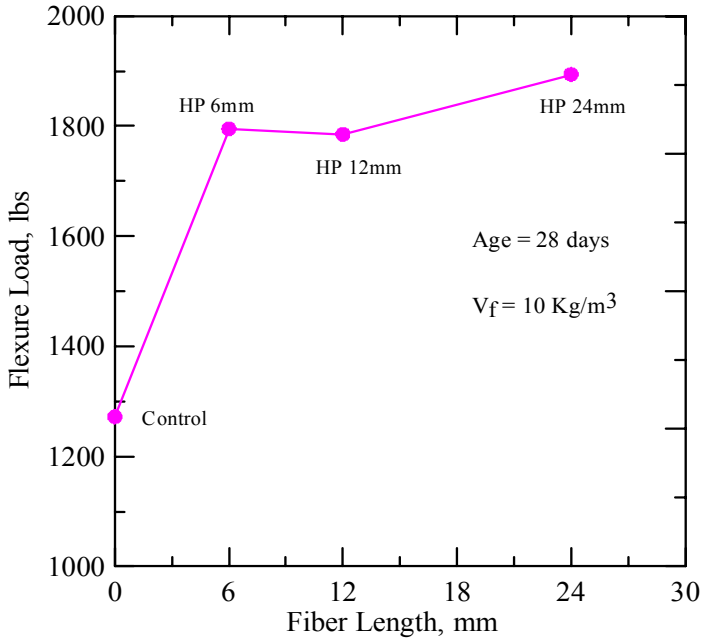

a) Effect of fiber lengths on flexural load

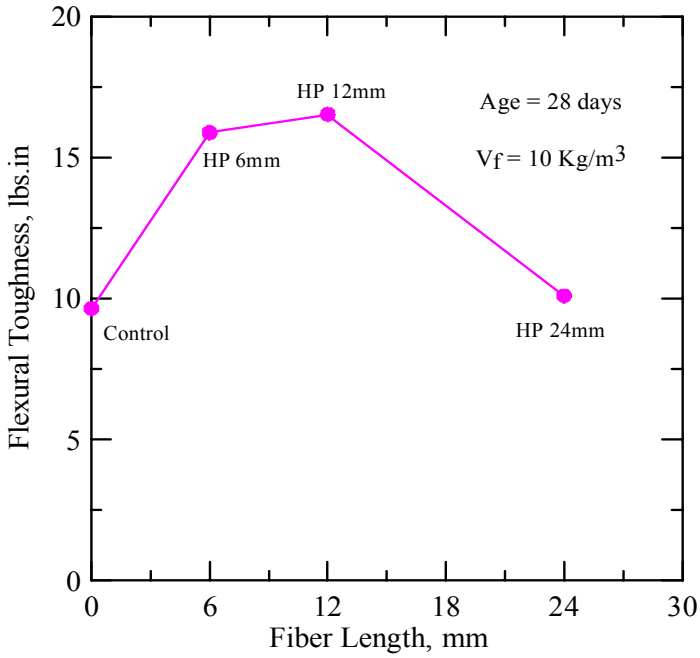

b) Effect of fiber lengths on flexural toughness

Figure 4.41. Effect of fiber lengths on the flexural properties of FRC

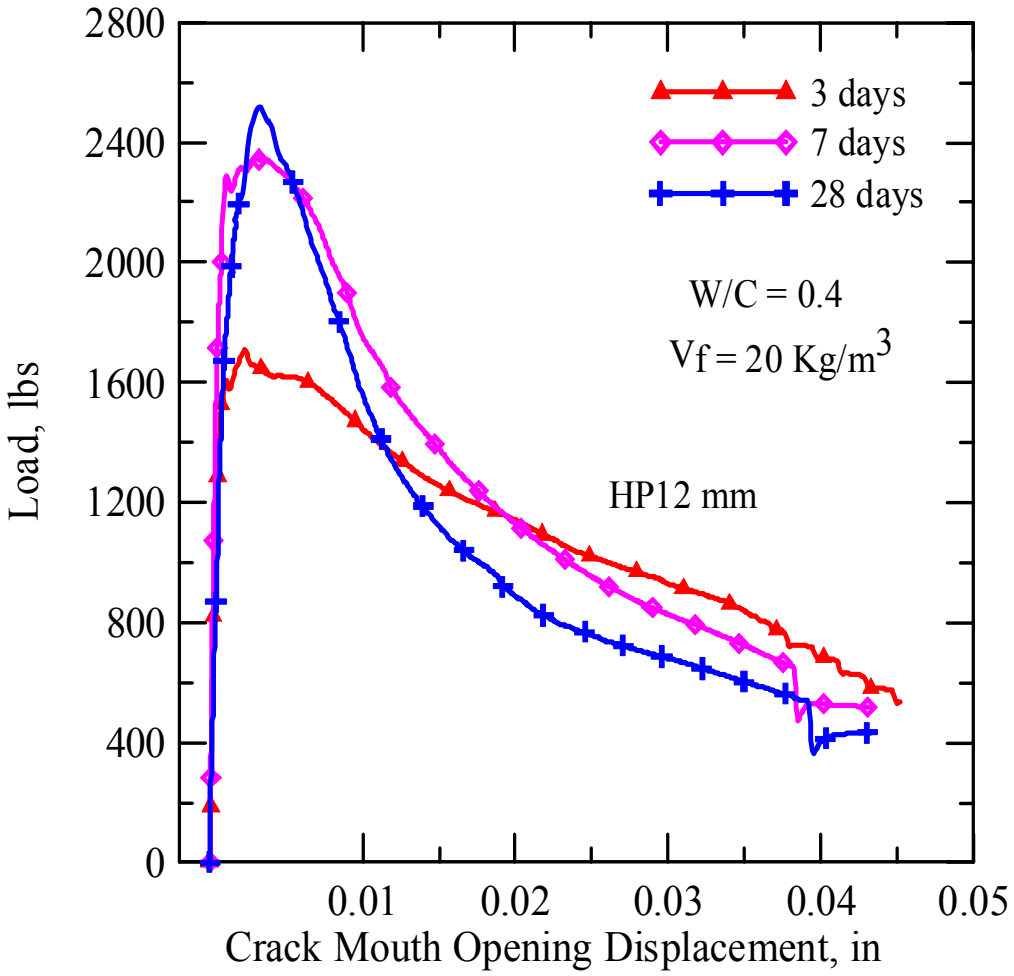

Figure 4.42. Load vs. CMOD for FRC with HP12 mm fibers with 20 Kg/m^3 at 3, 7 and 28 days

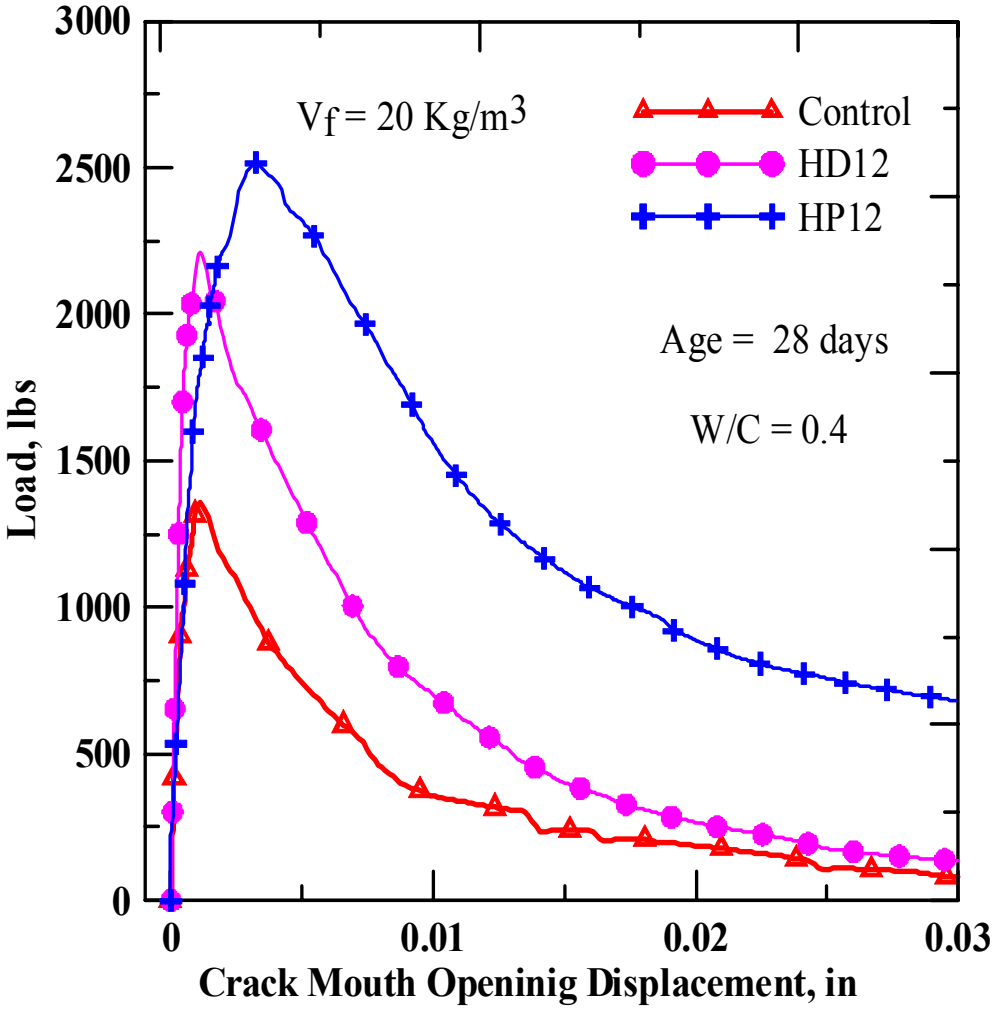

Figure 4.43. Comparison of flexural response of HP and HD fibers

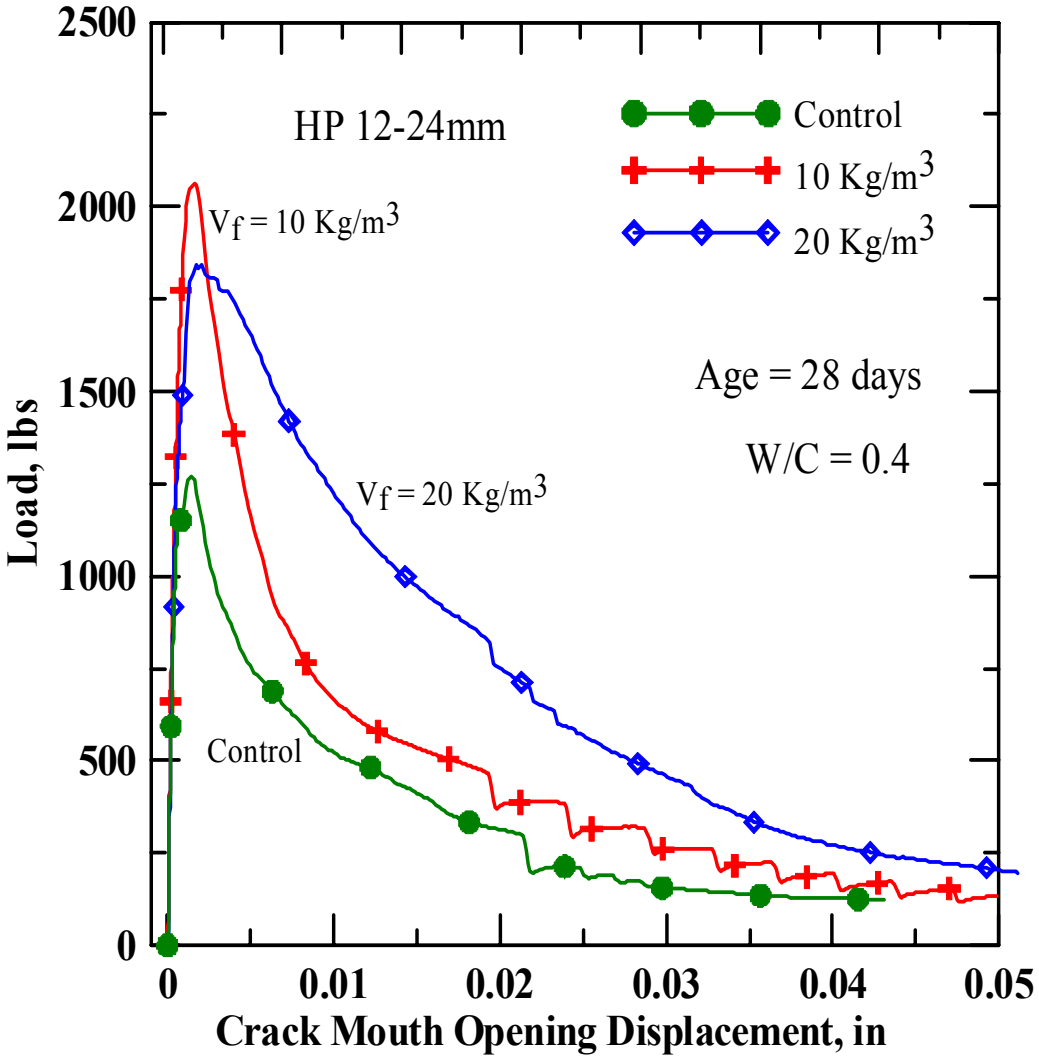

Figure 4.44. Effect of fiber volume fraction on FRC with HP12-24 (50%-50%) fibers

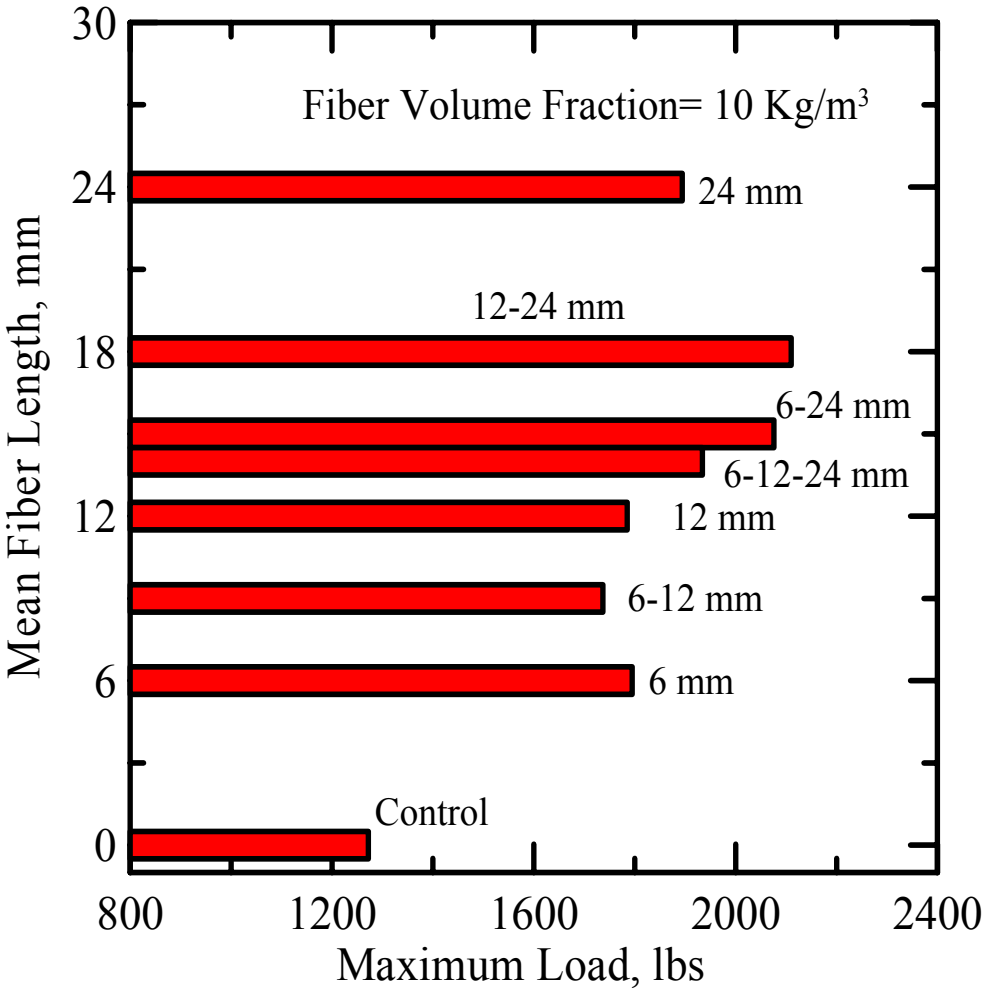

Figure 4.45. Bar graph showing the effect of mean fiber length on flexural loads

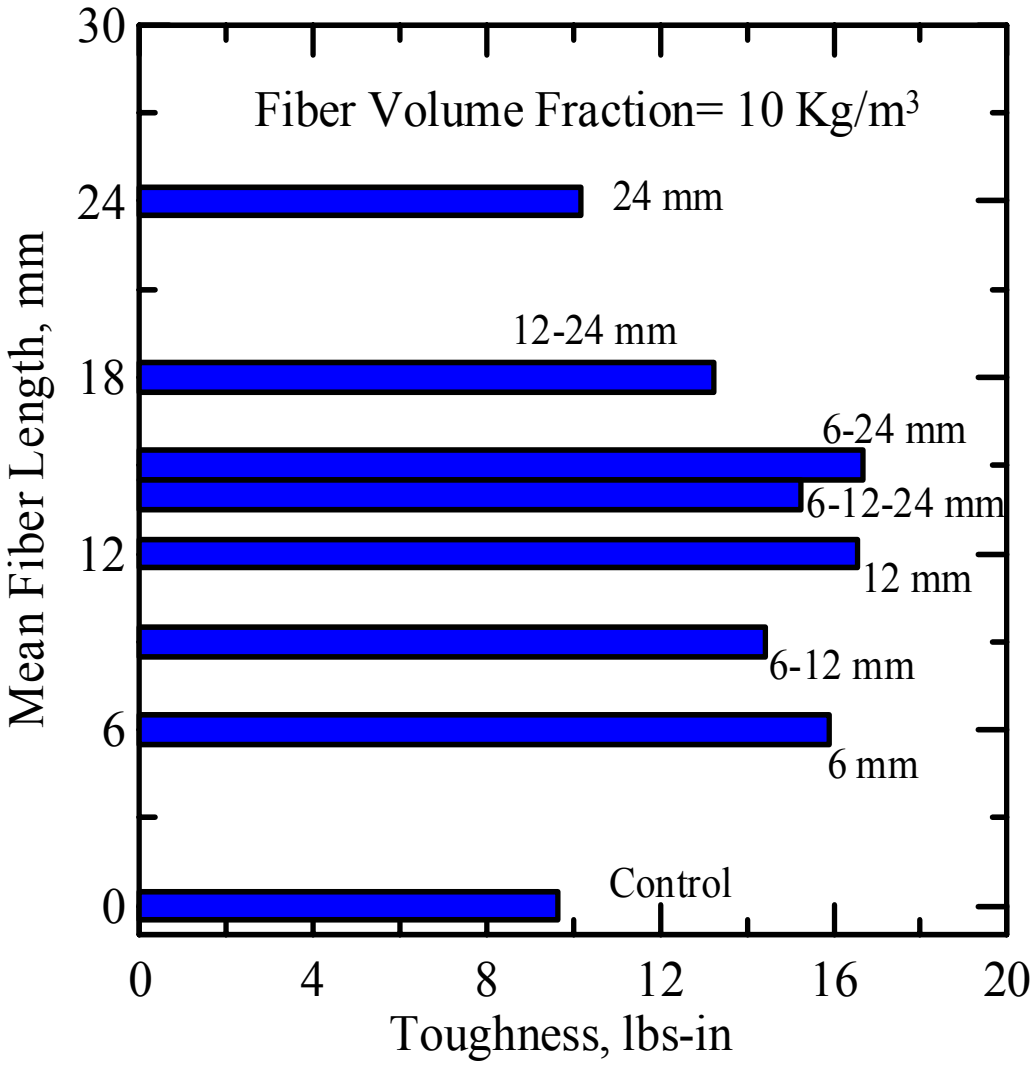

Figure 4.46. Bar graph showing the effect of mean fiber length on the toughness

CHAPTER 5

CONCLUSION

The following conclusions are drawn from the results obtained during this study:

5.1 Flyash Concrete

The study indicated that there is a great potential of using 30% flyash instead of the present guidelines of the Arizona Department of Transportation (ADOT) in which 20% flyash is used. It is possible to produce paving quality concrete mix up to 30% cement replacement with strength higher than 4000 psi which is the service level strength required for this class of concrete. The mix design resulted in considerable saving of the cement content in the concrete. The proposed mix design can save up to 40 lbs. of cement per Cu.yd of class P concrete when compared to the mix design used by the ADOT. The use of higher dosage of flyash is therefore quite favorable without any adverse effects on short term or long-term properties while resulting in considerable cost saving.

The test results indicated that the strength of the concrete with 30% flyash was higher than both the control concrete and the concrete containing 20% flyash. At 30% cement replacement, the strength exceeded 7000 psi, while the field trial samples exceeded 5000 psi level.

The specimen with 30% flyash and W/C ratio of 0.42 showed the highest amount of energy absorption. The flexural tests conducted for concrete with different superplasticizer contents indicated that there is an insignificant difference in flexure load capacity between the various concrete specimens. This means that the content of the superplasticizer does not significantly affect the mechanical performance of the concrete.

However, superplasticizer has significant effect on the rheology properties of the concrete, which can help with the workability of the fresh concrete.

5.2 *Concrete with AR Glass Fibers*

The study indicated that there is great potential in reinforcing the concrete material with AR Glass fibers from strengthening and toughening perspectives. The addition of fibers results in considerable increase in strength and toughness of Glass Fiber Reinforced concrete (GFRC). This was obtained for all fiber lengths used in the study.

The flexure test results indicated that the fiber volume fraction has significant effect on flexural properties of the FRC. The concrete with the HP12 mm fiber with the 20 Kg/m^3 fibers content exhibited 30% increase in the strength and 100% increase in the toughness compared to the 10 Kg/m^3 fibers content.

The fiber length has a significant effect on the flexural properties of the FRC. The test results indicated that increasing the fiber length increases the flexural load capacity. However, a significant reduction in the flexural toughness of nearly 40% was observed for the HP24 mm fiber concrete compared with the HP6 mm fiber concrete. For the hybrid systems, the concrete with the HP1224 mm length gave the optimal flexural behavior for the flexural load. Test results indicated that the increase in mean fiber length increasing the flexural load capacity. However, further increase in the average fiber length, resulted in a reduction of the toughness.

The compression test results indicated that the fiber volume fraction has significant effect on the compressive strength of the FRC. It was found that the concrete with the HP12 mm fibers with the dosage of 20 Kg/m^3 fibers exhibited 15% more

compressive strength than the 10 Kg/m^3 fibers. However, a significant reduction in the toughness of nearly 25% was observed.

REFERENCES

Neville, A. M. (1995). *Properties of Concrete* (4th ed.). London.

Carette, G., Bilodeau, A., Chevrier, R.L., & Malhotra, V.M. (1993). Concrete Incorporating High Volumes of Fly Ash. *ACI Materials Jounnal*, *90 (6)*, 535-544.

Naik, T. R., Ramme, B. W., & Tews J. H. (1995). Pavement Construction with High-Vloume Class C and Class F Fly Ash Concrete. *ACI Materials Jounnal*, *92 (2)*, 200-210.

Tixier, R., & Mobasher, B. (2000). Development and Application of high performance Concrete Materials with Blended Coal Flyash – Literature Review. *TECHNICAL REPORT* , *00-1*.

Frondistouyannas, S. (1977). Flexural Strength of Concrete with Randomly Oriented Glass Fibers. *Magazine of Concrete Research, 29 (100)*, 142-146.

Mobasher, B., & Shah, S. P. (1989). Test Parameters in Toughness Evaluation of Glass Fiber Reinforced Concrete Panels. *ACI Materials Jounnal*, *92 (2)*, 448-458.

Mobasher, B., & Li, C. Y. (1996). Mechanical Properties of Hybrid Cement Based Composites. *ACI Materials Jounnal*, *93 (3)*, 284-293.

Mane, S. A., Tixier, R., & Mobasher, B. (2001). Development and Application of High Performance Concrete Materials with Blended Coal Flyash. *Final Report Submitted to SRP.*

Sakai, M., & Bradt, R. C. (1986). Graphical Methods For Determining the Nonlinear Fracture Parameters of Silica and Graphite Refractory Composites. *Fracture Mechanics of Ceramics, 7*, 127-142.

Ouyang, C., Mobasher, B., & Shah, S. P. (1990). An R- Curve Approach for Fracture of Quasi-Brittle Materials. *Engineering Fracture Mechanics, 37*, 284-293.

Arino, A., Li, C. Y., & Mobasher, B. (1995). Experimental R- Curve for Assessment of Toughening in Fiber Reinforced Cementitious Composites. *ACI SP, 155 (5)*, 93-114.

APPENDIX A

MODEL FIT CURVES

R-Curve Analysis using Compliance Approach

It is generally accepted that due to existence of a relatively large fracture process zone, which results in the stable crack propagation, LEFM cannot be directly applied to cement-based composites. One alternative is to conduct a stable three-point bend test on a notched beam to obtain a continuous load-deflection curve. This curve is further used to obtain the fracture energy as the area under the curve. A primary characteristic in fracture is the existence of stable crack growth prior to the crack reaching its critical length. The length of process zone depends on microstructure (size of aggregate) as well as on the geometry of the specimens. R-Curves present a methodology to characterize the fracture and take into account the effect of geometry, material properties, and the size of the process zone.

R-Curve models integrate the energy dissipation in the process zone as a toughening component of the matrix material. Approaches that are based on the energy principle and the unloading-reloading methods have been quite convenient for evaluating nonlinear fracture toughness parameters as a function of crack length (Sakai & Bradt, 1986). These ideas relate the energy dissipation in the process zone to an effective elastic crack length. C. Ouyang, B. Mobasher and S. P. Shah (1990) studied the influence of geometry on the R-Curves and on other characteristics of the fracture response. An experimental procedure was developed for the measurement of R-Curves based on loading-unloading curves (Arino, Li, & Mobasher, 1995).

The strain energy release rate, G, represents the energy available for incremental crack extension. Once it reaches a critical value G_{IC}, an instability condition is reached

and crack propagation occurs. To characterize fracture toughness using a single parameter G_{IC}, only the peak load of a notched specimen tested under mode I condition is required. Quasi-brittle materials dissipate energy due to frictional sliding, aggregate interlock, and crack surface tortuosity. After an initiated crack begins to propagate, the dissipating mechanisms evolve. The increase in the apparent toughness can be related to the stable crack growth by means of an R-Curve. The condition for stable crack growth is:

$$G(a) = R(a) \qquad \frac{\partial G(a)}{\partial a} < \frac{\partial R(a)}{\partial a} \tag{1}$$

The condition for crack instability can be defined as:

$$G(a_c) = R(a_c) \qquad \frac{\partial G}{\partial a} = \frac{\partial R}{\partial a} \quad @\, a = a_c \tag{2}$$

The procedure for calculation of R-Curves using the compliance approach for loading unloading cycles is as follows: A closed loop control test is conducted on a three point specimen with geometrical dimensions b, t, a_0, and S representing the depth, thickness, initial notch length, and span. Several cycles of loading unloading are recorded and the load vs. deformation data is collected. Three measurements were taken for each loop of loading unloading representing the load (P) where the unloading of a cycle starts, the compliance (C_u) for each unlading curve, and displacement (u) at a point where each loop ends. Sets of three readings were used as an input to calculate the R-Curve and its parameters. First the experimentally measured compliance is used to calculate the crack extension Δa for that cycle according to equation 3. From the initial first loading curve ($\Delta a = 0$) the Modulus of Elasticity (E) is calculated and used for future calculations.

$$C_u = \frac{6\,S\,(a_0 + \Delta a)\,V(\alpha)}{E\,b^2\,t}\ ,\ \alpha = \frac{a_0 + \Delta a}{b} \tag{3}$$

Next, the rate of change of compliance can be used to obtain the strain energy release rate as shown in equation 4. The compliance is plotted as a function of the crack extension and a curve fit algorithm is applied to fit the response. Numerical differentiation of the compliance-crack length results in an average value of the rate since several compliance measures are used to calculate the rate. In the presence of residual displacements, additional terms are needed to account for the rate of change of inelastic displacement with respect to crack growth as well. Once all the parameters are obtained, the results are compiled according to equation 4.

$$G^*(a) = \frac{1}{2\,t}\frac{\partial C}{\partial a}P^2 + \frac{1}{2\,t}\frac{\partial \delta_r}{\partial a}P \tag{4}$$

The R curve is then obtained using the well-known relationship of equation (5).

$$K^R(a) = \sqrt{E_c'\,G^*(a)} \tag{5}$$

Where, $E'_c = E_c / (1 - \upsilon_c^2)$ for plane strain and E_c for plane stress. E_c and υ_c represent the elastic modulus and the Poisson's ratio. The R-Curve is plotted as a function of the incremental crack growth.

Fracture Response Predicted from R-curves

Fracture response of a specimen, including load-CMOD and load-displacement curves can be predicted by the use of the R-curve. The Math lab program is developed which is simulating closed loop Three-point bending test conducted in the laboratory and

generate the theoretical load-CMOD and load-displacement curve based on the standard value of Stress intensity factor (K_{ic}) and Crack tip opening displacement ($CTOD_c$) for the particular material.

Figure A.1 presents the theoretical fitting of load-CMOD curve generated from program with the actual experimental curve. The above curve also contains the input parameter used to generate the theoretical curve. A good agreement between the experimental results and theoretical prediction is observed with good match for pre peak and initial post peak response. Figures A.2, A.3, A.4 and A.5 show the influence of flyash on the R-curve. Figures A.6 and A.7 presents the theoretical fitting of load-CMOD curve generated from program with the experimental curve of the field samples.

Figure A.8 present the crack length vs. fracture resistance curve for 30% fly ash in concrete at 28 days with different superplasticizer contents and w/c ratio. From the graph it can be observed that there is no significant difference in values of fracture resistance for low and high superplasticizer contents. The W/C ratio has clear effect with low W/C ratio has higher value of fracture resistance R than high water cement ratio. The concrete with 30% flyash and with low superplasticizer and low W/C has highest value of fracture resistance of 0.17 psi*$in^{1/2}$, which indicate that it has better post peak response with better ductility and energy absorption capacity than other mix. A summery of results of R-curve analysis is shown in Table A.1.

Table A1

R-Curve Results

Mix ID	Modulus of Elasticity E	Poisson's Ratio	Stress Intensity Factor K^S_{Ic}	Crack Tip Opening Displacement Ctodc
	psi		psi*in $^{1/2}$	in
L30_42_LS	2.10E+06	0.25	1381.44	1.97E-03
L30_42_HS	1.74E+06	0.20	1266.32	1.97E-03
L35_42_LS	2.10E+06	0.20	1323.88	1.97E-03
L30_45_LS	1.74E+06	0.21	1295.10	1.97E-03
L30_45_HS	1.89E+06	0.22	1266.32	1.97E-03
TRM_SRP_30FA	2.10E+06	0.25	1323.88	1.97E-03
TRM_20FA	2.10E+06	0.22	1352.66	1.97E-03

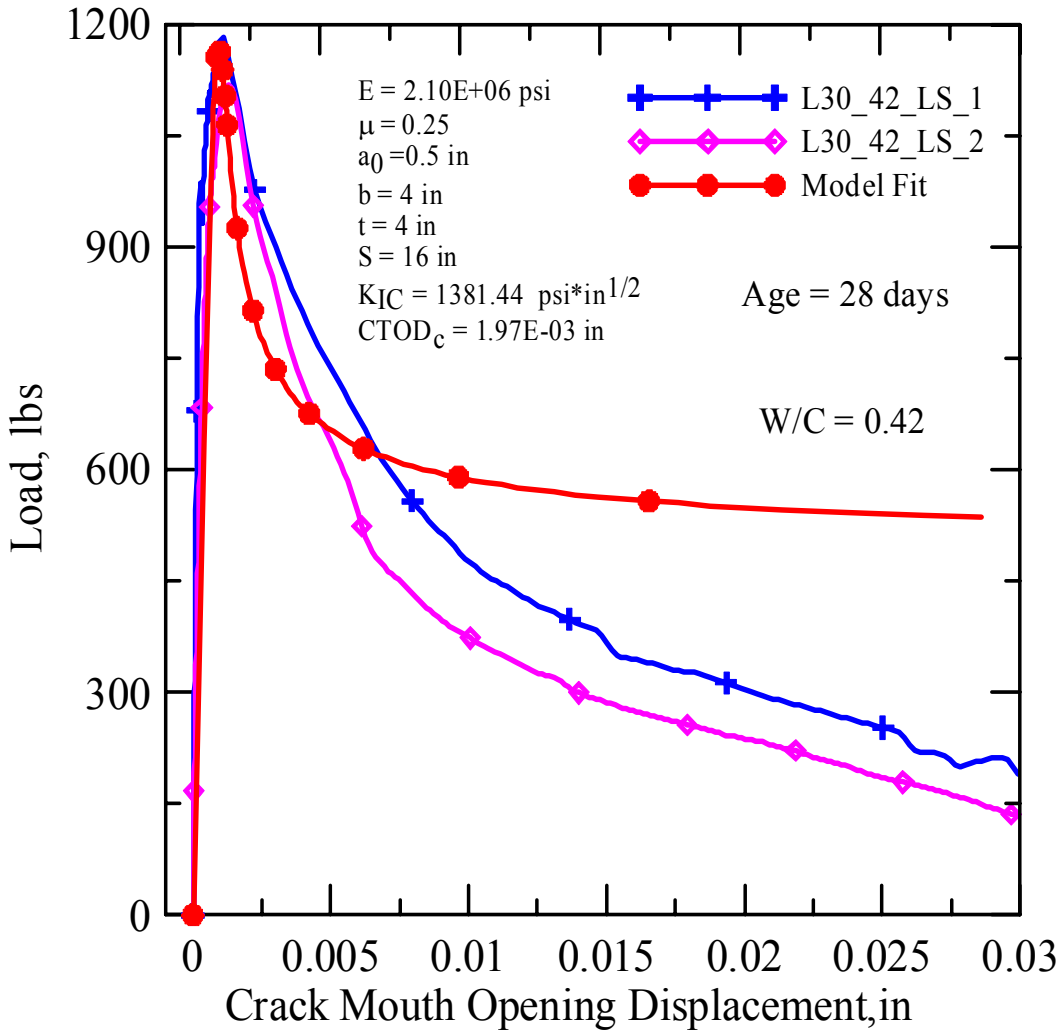

Figure A1. Model fit curve for Load vs. CMOD for 30% flyash in concrete with low superplasticizer and 0.42 w/c ratio

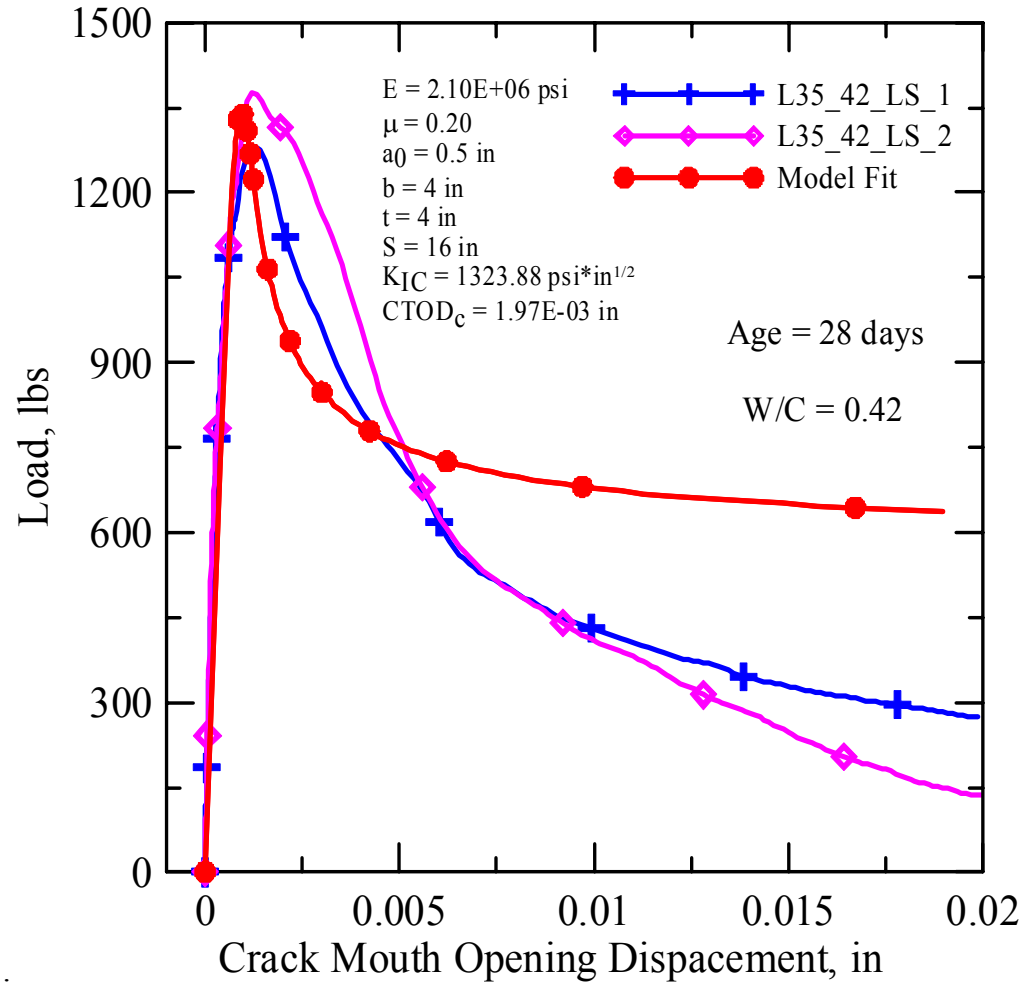

Figure A2. Model fit curve for Load vs. CMOD for 35% flyash in concrete with low superplasticizer

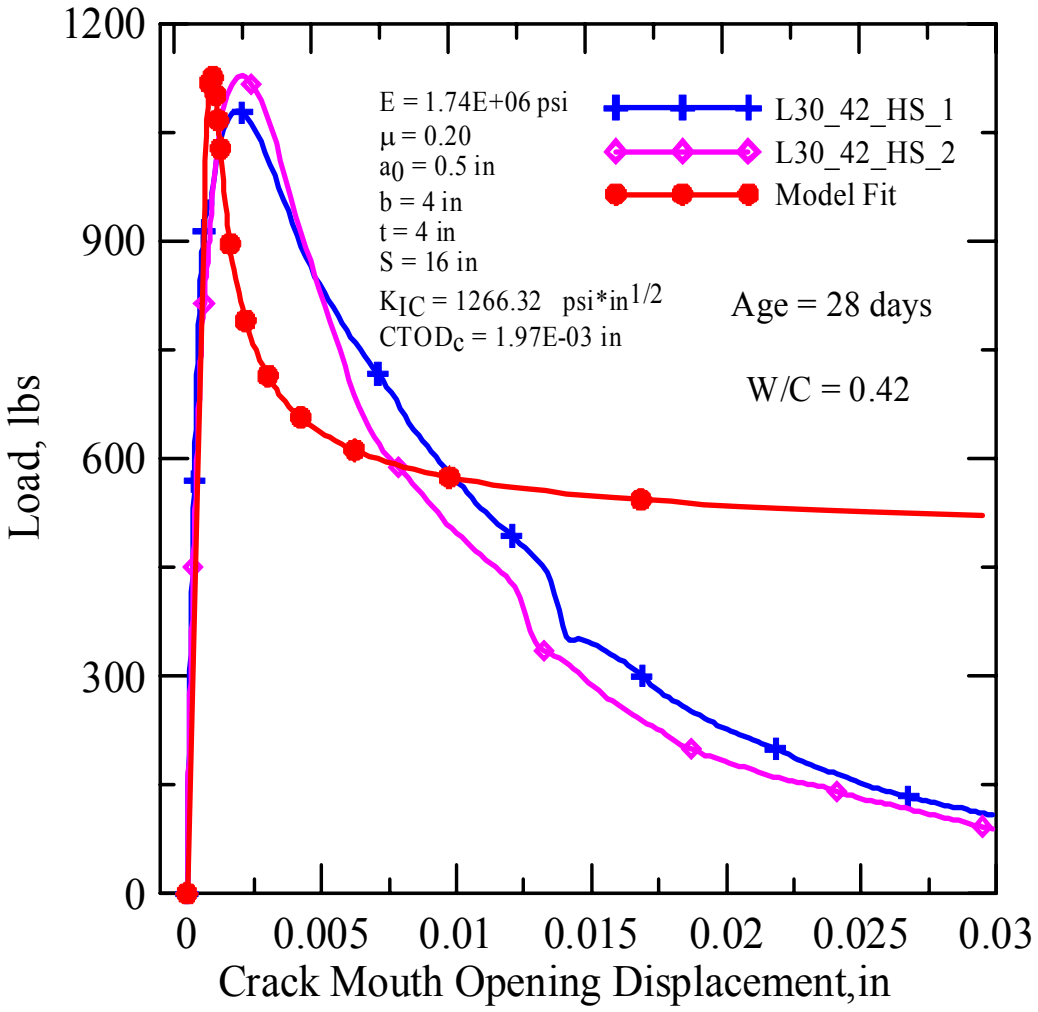

Figure A3. Model fit curve for Load vs. CMOD for 30% flyash in concrete with high superplasticizer

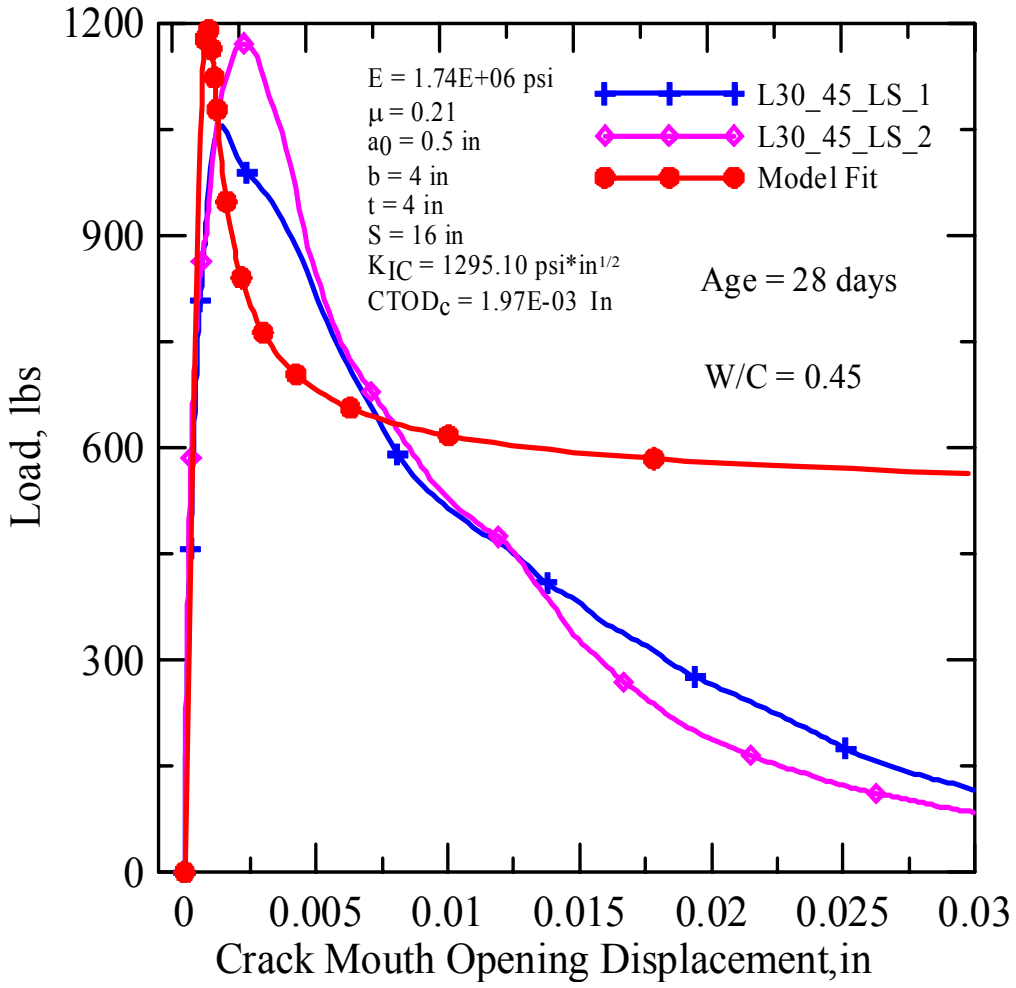

Figure A4. Model fit curve for Load vs. CMOD for 30% flyash in concrete with low superplasticizer and 0.45 w/c ratio

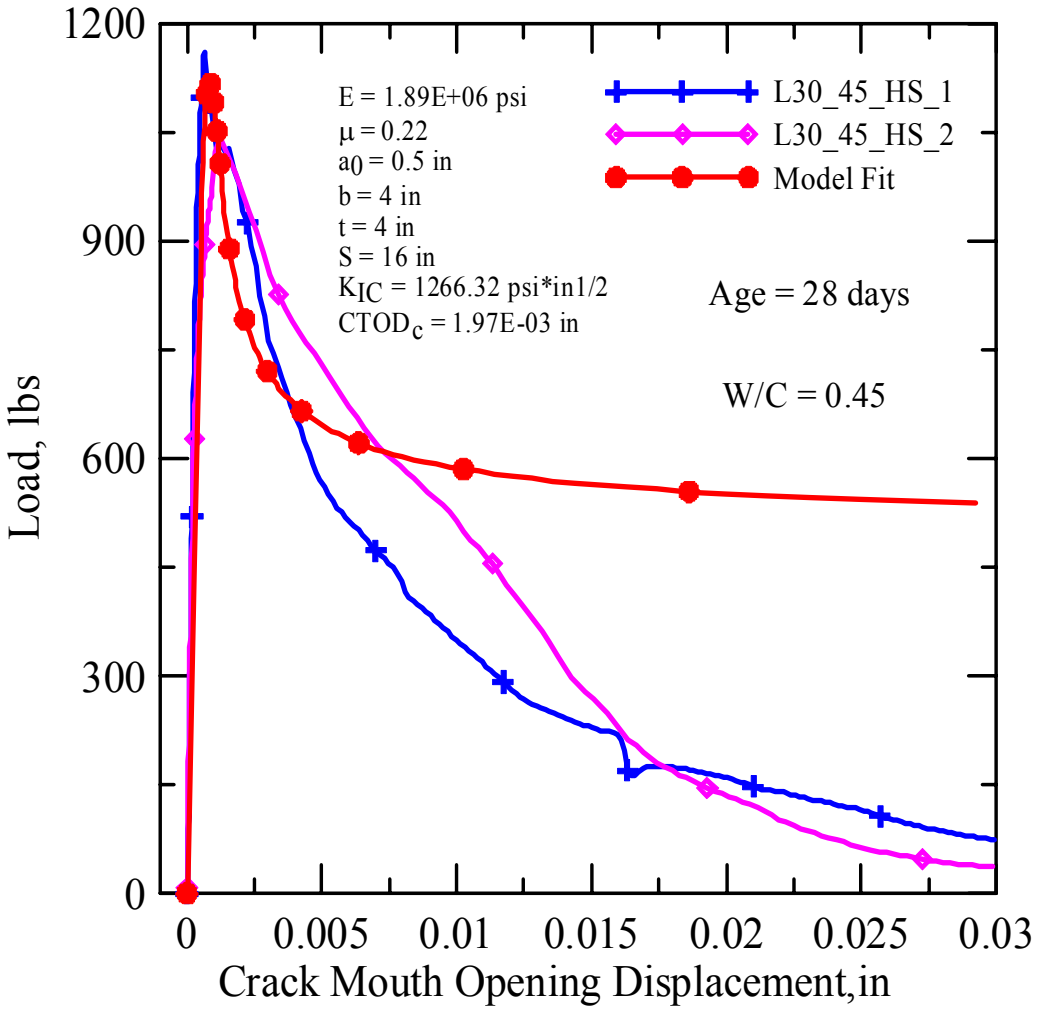

Figure A5. Model fit curve for Load vs. CMOD for 30% flyash in concrete with low superplasticizer and 0.45 w/c ratio

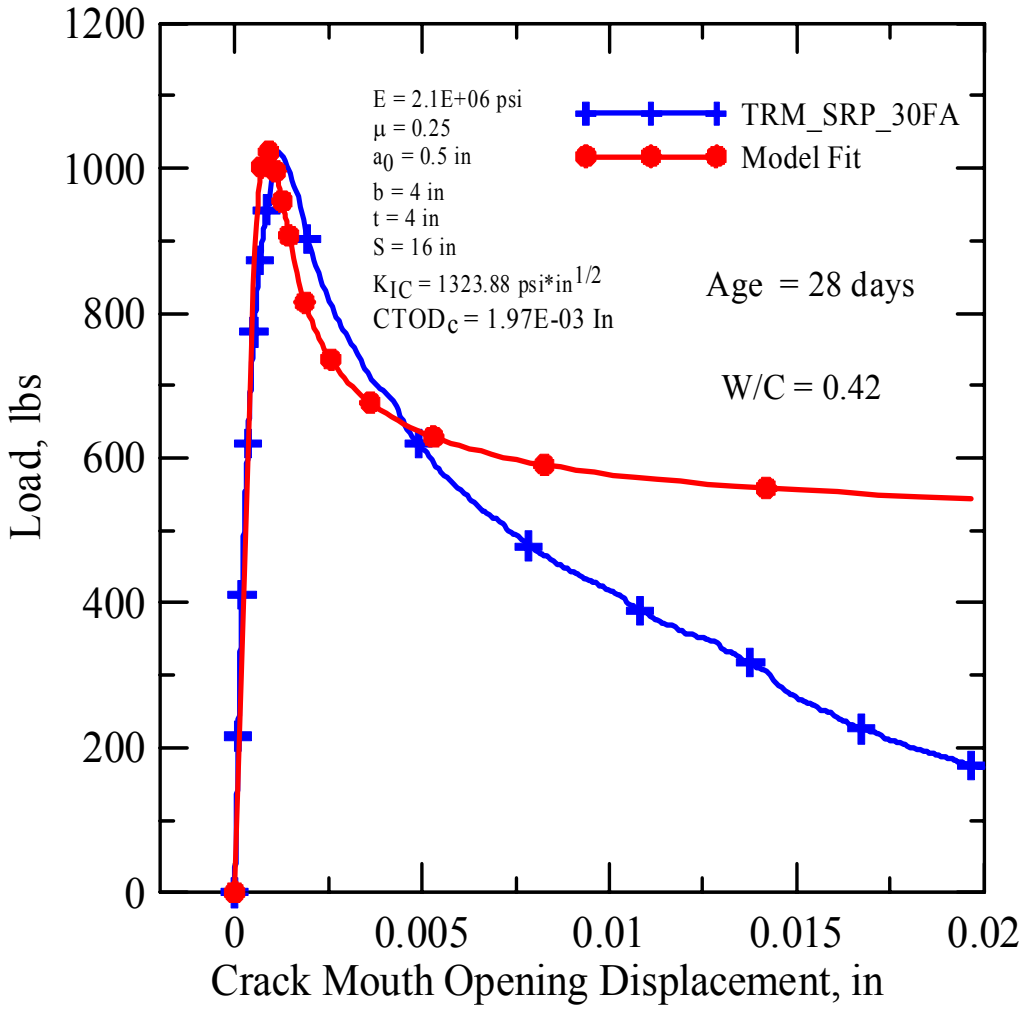

Figure A6. Model fit curve for Load vs. CMOD for SRP 30% flyash in concrete with 0.42 w/c

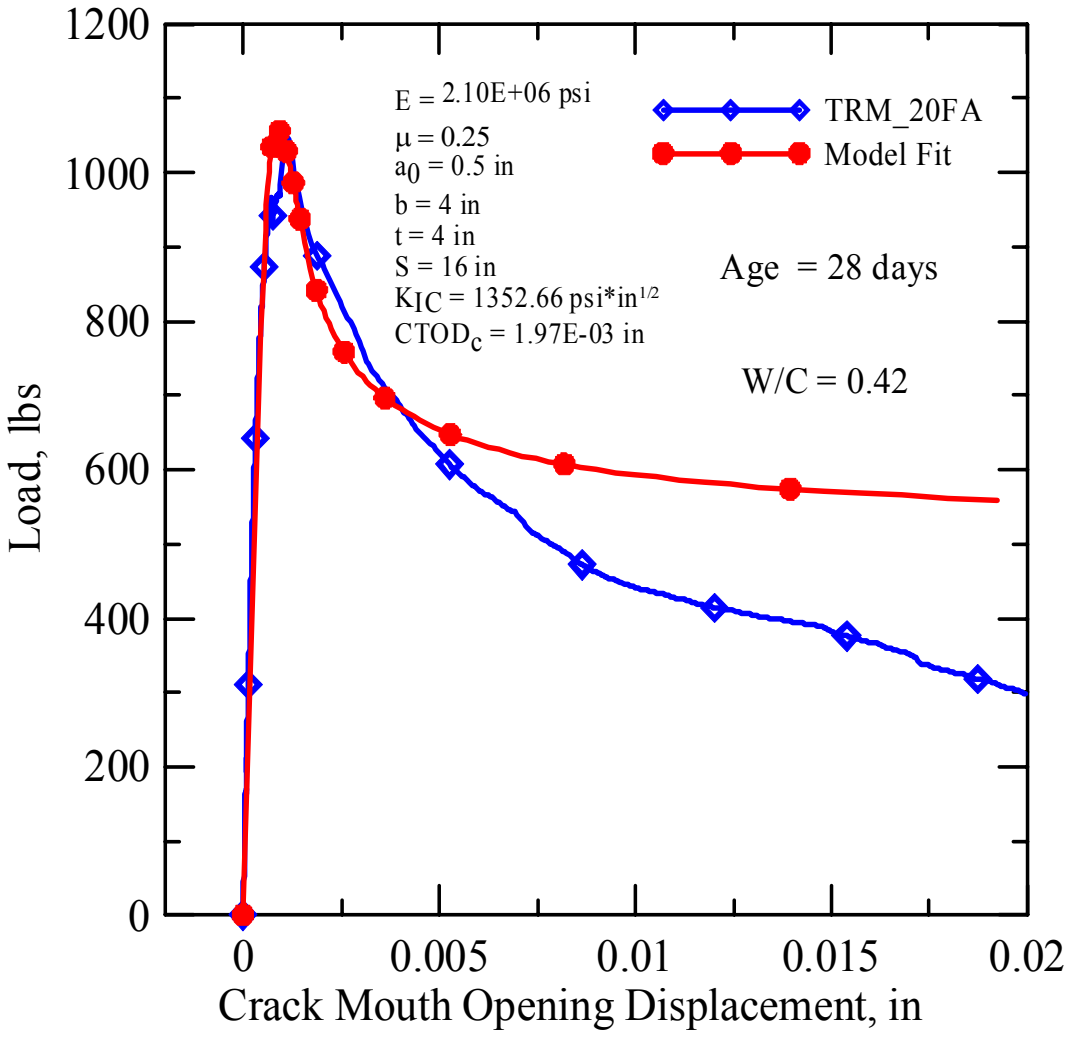

Figure A7. Model fit curve for Load vs. CMOD for 20% flyash in concrete with 0.42 w/c.

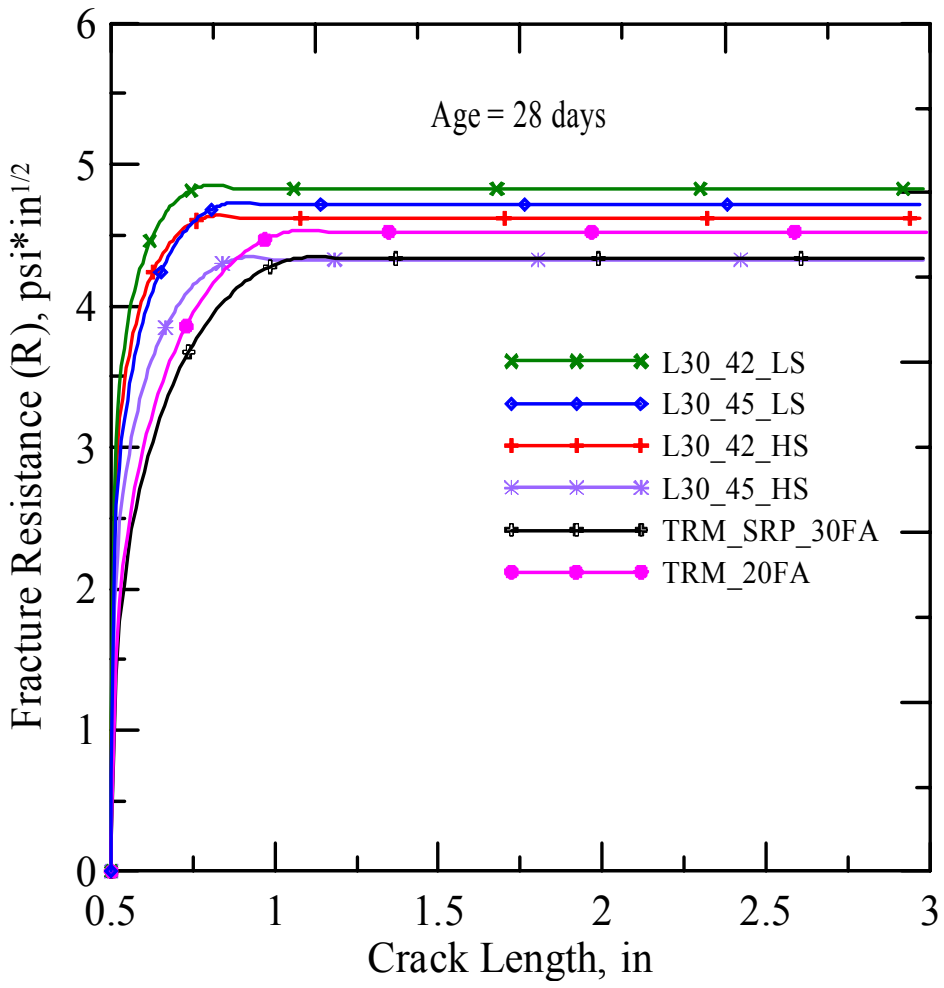

Figure A8. Crack length vs. Fracture Resistance R for concrete with different superplasticizer content and water cement ratio

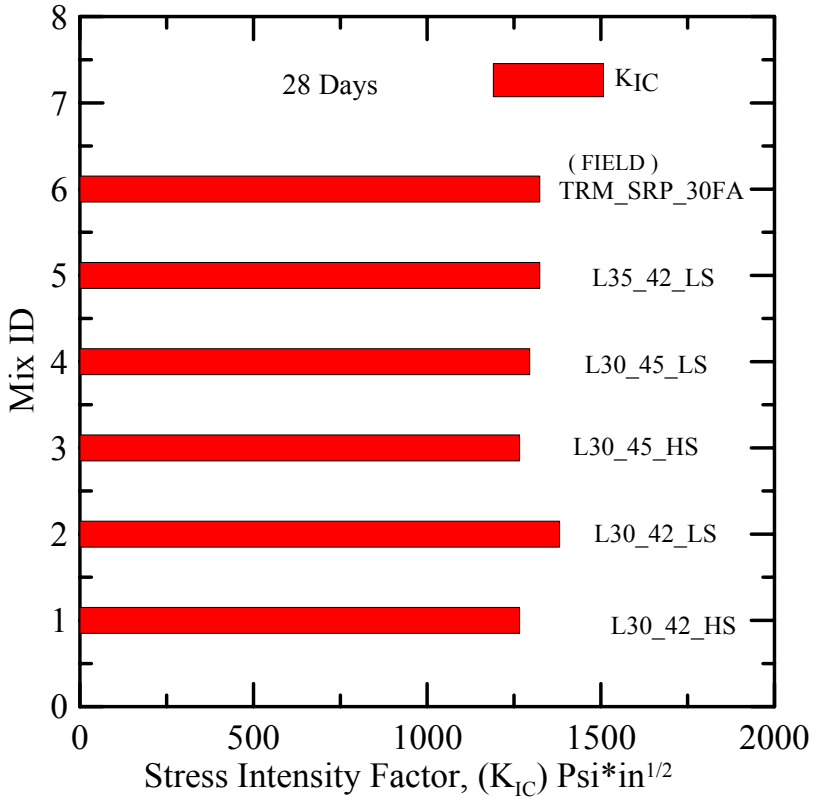

Figure A9. Comparison of Stress Intensity Factor for various mixes